𝔓𝔞𝔨𝔦𝔰𝔱𝔞𝔫 𝔍𝔬𝔲𝔯𝔫𝔞𝔩 𝔬𝔣 𝔖𝔱𝔞𝔱𝔦𝔰𝔱𝔦𝔠𝔰 𝔞𝔫𝔡 𝔒𝔭𝔢𝔯𝔞𝔱𝔦𝔬𝔫 𝔕𝔢𝔰𝔢𝔞𝔯𝔠𝔥

A New Compound Lomax Model: Properties, Copulas, Modeling and Risk Analysis Utilizing the Negatively Skewed Insurance Claims Data

Mohamed S. Hamed[1,2], Gauss M. Cordeiro[3],
and Haitham M. Yousof[2,*]

* Corresponding Author

[1]Department of Computer Sciences and Information, Gulf Colleges, Saudi Arabia, mssh@GULF.EDU.SA
[2]Department of Statistics, Mathematics and Insurance, Benha University, Benha 13518, Egypt,
mohamed.hamed@fcom.bu.edu.eg & haitham.yousof@fcom.bu.edu.eg
[3]Universidade Federal de Pernambuco, Departamento de Estatística, Brazil. gauss@de.ufpe.br

Abstract

Analyzing the future values of anticipated claims is essential in order for insurance companies to avoid major losses caused by prospective future claims. This study proposes a novel three-parameter compound Lomax extension. The new density can be "monotonically declining", "symmetric", "bimodal-asymmetric", "asymmetric with right tail", "asymmetric with wide peak" or "asymmetric with left tail". The new hazard rate can take the following shapes: "J-shape", "bathtub (U-shape)", "upside down-increasing", "decreasing-constant", and "upside down-increasing". We use some common copulas, including the Farlie-Gumbel-Morgenstern copula, the Clayton copula, the modified Farlie-Gumbel-Morgenstern copula, Renyi's copula and Ali-Mikhail-Haq copula to present some new bivariate quasi-Poisson generalized Weibull Lomax distributions for the bivariate mathematical modelling. Relevant mathematical properties are determined, including mean waiting time, mean deviation, raw and incomplete moments, residual life moments, and moments of the reversed residual life. Two actual data sets are examined to demonstrate the unique Lomax extension's usefulness. The new model provides the lowest statistic testing based on two real data sets. The risk exposure under insurance claims data is characterized using five important risk indicators: value-at-risk, tail variance, tail-value-at-risk, tail mean-variance, and mean excess loss function. For the new model, these risk indicators are calculated. In accordance with five separate risk indicators, the insurance claims data are employed in risk analysis. We choose to focus on examining these data under five primary risk indicators since they have a straightforward tail to the left and only one peak. All risk indicators under the insurance claims data are addressed for numerical and graphical risk assessment and analysis.

1. Introduction

Every property/casualty claim procedure uses two independent random variables (RVs): the claim-size RV and the claim-count RV. The first two basic claim RVs can be combined to produce the aggregate-loss RV, which represents the total claim amount generated by the underlying claim procedure. In this study, a unique distribution of claim-size variables known as the quasi-Poisson generalized Weibull Lomax (QPGWL) model is discussed. Several actuaries employed a wide variety of parametric families of continuous distributions to simulate the size of property and casualty insurance claim amounts. Claim-size RVs take only non-negative values. Thus, for all such RVs $\Pr\{Z < 0\} = 0$, i.e.,

$F_Z(z) = 0$ for all $Z < 0$. The probability density function (PDF) $f_Z(z)$ for a continuous size-of-loss model for which claim size is unbounded (or unlimited) from above takes on positive values over a semi-infinite interval of the form $0 \le d_1 < Z < \infty$. For positive d_2 in this interval, the portion of the distribution defined on the sub-interval (d_2, ∞) is called the long tail of the distribution. Alternatively, the part of the loss distribution defined on (d_1, d_2), extending to the left and bounded below by 0, is called the short tail of the distribution. Clearly, such probability distributions cannot be symmetric.

Due to the actuarial literature, the insurance claim-size data sets frequently have positive skewness. However, this article examines and models a new collection of insurance claims data that is adversely skewed under the QPGWL model and some risk indicators. An actuarial measurement of the potential loss that might happen in the future as a result of a specific action or event is the risk exposure. As part of a review of the business's risk exposure, risks are usually ranked according to their likelihood of occurring in the future multiplied by the potential loss if they did. The insurance firms can differentiate between little and large losses by ranking the likelihood of likely losses in the future. Speculative risks frequently result in losses such as failures to comply with regulations, a decline in brand value, security flaws, and liability issues. Generally, the risk exposure (r(·)) can be expressed as

$$r(\cdot) = TL \times \Pr(\cdot),$$

where TL is the total loss of risk occurrence and $\Pr(\cdot)$ refers to the probability of the occurring risk. However, there has been a lot of work done to examine historical insurance data using time series analysis or continuous distributions. Recently, numerous actuaries have represented actual insurance data using continuous distributions, particularly those with large tails.

Real data have been modelled using continuous heavy-tailed probability distributions in a variety of practical domains, including economics, engineering, risk management, dependability, and actuarial sciences. The insurance data sets can be unimodal right-skewed, right-skewed with heavy tails, or left-skewed. In this paper, we show how the flexible continuous heavy-tailed QPGWL distribution can be utilized to represent left-skewed insurance claims data.

The insurance claims data present a variety of challenges despite huge significance. The largest issue with risk analysis and its applicable applications is identifying the quality of the data and calculating the number of incomplete or missing observations; see Hogg and Klugman (1984), Lane (2000), Stein et al. (2014), and Ibragimov and Prokhorov (2017). Although, the real data sets for insurance claims are typically positive and frequently include right tails or heavy right tails, we will deal with negatively skewed insurance claims data. What allowed us to do this is that the new distribution is flexible enough for accommodating and modeling this type of data.

Many studies employed the Lomax and lognormal distributions to model insurance payments data, and more specifically, massive insurance claim payment data. Several scholars, including Resnick (1997), have used the generalized Lomax model. Due of its monotonically decreasing density shape, the Lomax model does not offer a good fit for many actuarial applications when the frequency distributions are hump shaped. So, the lognormal is frequently used to model these data sets in these circumstances. However, this model does not have enough flexibility to deal with negatively skewed actuarial data sets. In this work, we present the QPGWL distribution for the left-skewed insurance claims real data sets to overcome this problem in the old standard models. As will be explained in more details and plots, it is noted that the probability density function (PDF) of the QPGWL model can be "monotonically decreasing", "asymmetric with right tail", "asymmetric with wide peak", "asymmetric with left tail", "symmetric" and "bimodal-asymmetric". All these characteristics motivate the QPGWL distribution to model the insurance claims data and study and analyze risks accordingly.

In order to model the real-life data of business failure, econometrics, actuarial science, queueing theory, and internet traffic modelling, Lomax (1954) investigated his continuous heavy-tail probability distribution. In many research papers, the Lomax model is called Pareto type-II (Pa-II) distribution. Special efforts aim to expand the Lomax distribution and its relevant extensions in applied statistics and related fields such as engineering, instance, wealth inequality, income, medicine, biological studies, and reliability. The Lomax model is applied for modeling real data of income and wealth (Harris,1968; Asgharzadeh and Valiollahi, 2011), type-II progressive censored competing risks data (Cramer and Schemiedt, 2011), real data of firm sizes (Corbellini et al., 2007)), reliability analysis, engineering, taxes and economic (Elgohari and Yousof, 2020a), times of failure/survival (Chesneau and Yousof, 2021), among others. Further, many other Lomax extensions can be cited such as the exponentiated Lomax and gamma Lomax (Gupta et al., 1998; Cordeiro et al., 2015), the transmuted Topp-Leone Lomax (Yousof et al., 2017), Kumaraswamy

Lomax (Lemonte and Cordeiro, 2013), Burr-Hatke Lomax (Yousof et al., 2018b), beta Lomax (Lemonte and Cordeiro, 2013), odd log-logistic Lomax (Elgohari and Yousof, 2020a), proportional reversed hazard rate Lomax distribution (Elgohari and Yousof, 2020) and special generalized mixture Lomax (Chesneau and Yousof, 2021). Other important and flexible extensions can be found in Mansour et al. (2020e) and Aboraya et al. (2022).

A random variable has the Lomax distribution if its cumulative distribution function (CDF) is given by

$$F_\pi(y) = 1 - (1 + z)^{-\pi}|_{z \geq 0},$$

where $\pi > 0$ is the shape parameter. The above CDF of the one-parameter Lomax distribution is a special case from the Burr type XII (BXII) model. Hence, many theoretical details about the Lomax model and its relationship with other related distributions can be found in Burr (1942, 1968 and 1973), Lomax (1954), Burr and Cislak (1968), Harris (1968), Rodriguez (1977), Tadikamalla (1980) and Yadav et al. (2020).

We propose and study a new compound version Lomax (L) distribution using the generalized Weibull Lomax (GWL) model. The CDF of the three-parameter GWL model can be expressed as

$$\mathbf{G}_{a,b,\pi}(z) = (1 - exp\{-[(1 + z)^\pi - 1]^b\})^a|_{z \in \mathbb{R}^+}, \tag{1}$$

where $a, b, \pi > 0$ are three shape parameters. For $a = 1$, the GWL model reduces to the Weibull Lomax. For $b = 1$, it becomes the generalized exponential Lomax. For $b = 2$, it refers to the generalized Rayleigh Lomax. For $a = b = 1$, it is the exponential Lomax. For $a = 1$ and $b = 2$, the GWL model refers to the Rayleigh Lomax. For $\pi = 1$, it reduces to the exponentiated Weibull. For $a = \pi = 1$, it is just the Weibull. For $b = \pi = 1$, it is the exponentiated exponential. For $b = 2$ and $\pi = 1$, the GWL model is equal to the exponentiated Rayleigh. Consider the CDF of the quasi-Poisson family

$$F(z) = \frac{1}{1 - exp(-1)}\left\{1 - \frac{1}{exp[\mathbf{G}_{\underline{\mathbf{V}}}(z)]}\right\}, \tag{2}$$

where $\mathbf{G}_{\underline{\mathbf{V}}}(z)$ is the CDF of the baseline model, $\underline{\mathbf{V}}$ is the parameter vector, and let $\mathbf{G}_{\underline{\mathbf{V}}}(z) = \mathbf{G}_{a,b,\pi}(z)$. The CDF of the new model has the form

$$F_{a,b,\pi}(z) = \frac{1}{1 - exp(-1)}\{1 - exp[-(1 - exp\{-[(1 + z)^\pi - 1]^b\})^a]\}|_{a,b,c,z \in \mathbb{R}^+}, \tag{3}$$

Equation (3) defines the quasi-Poisson generalized Weibull Lomax (QPGWL) model. For $b = 1$, the QPGWL distribution reduces to the quasi-Poisson generalized exponential Lomax. For $b = 2$, it is the quasi-Poisson generalized Rayleigh Lomax. For $a = 1$, it becomes the quasi-Poisson Weibull Lomax. For $a = b = 1$, the QPGWL distribution becomes the quasi-Poisson exponential Lomax. For $b = 2$ and $a = 1$, it is the quasi-Poisson exponential Lomax. For $\pi = 1$, the QPGWL model refers to the quasi-Poisson generalized Weibull. For $\pi = b = 1$, it becomes the quasi-Poisson generalized exponential. For $\pi = 1$ and $b = 2$, it reduces to the quasi-Poisson generalized Rayleigh. For $\pi = a = 1$, it is equal to the quasi-Poisson Weibull. For $\pi = a = b = 1$, it becomes the quasi-Poisson exponential. For $b = 2$ and $\pi = a = 1$, it refers to the reduced quasi-Poisson exponential. By differentiating (3), the PDF follows as

$$f_{a,b,\pi}(z) = \frac{ab\pi \, exp\{-[(1 + z)^\pi - 1]^b\} \, exp[-(1 - exp\{-[(1 + z)^\pi - 1]^b\})^a]}{[1 - exp(-1)](1 + z)^{1-b\pi}[1 - (1 + z)^{-\pi}]^{1-b}(1 - exp\{-[(1 + z)^\pi - 1]^b\})^{1-a}}. \tag{4}$$

The hazard rate function (HRF) of the QPGWL extension can be obtained from $f_{a,b,\pi}(z)/[1 - F_{a,b,\pi}(z)]$. Let $Z \sim$QPGWL (a, b, π) be a RV having PDF (4). Figure 1 (left plot) provides some plots of the QPGWL PDF for selected parameters values. Figure 1 (right plot) gives some plots of the QPGWL HRF. Figure 1 shows that the PDF of the QPGWL model can be "monotonically decreasing", "asymmetric with right tail", "asymmetric with wide peak", "asymmetric with left tail", "symmetric" and "bimodal-asymmetric". Based on Figure 2, the HRF of the QPGWL

distribution can be "decreasing-constant", "upside down-constant", "increasing", "**J**-shape", "bathtub (**U**-shape)" and "upside down- increasing".

For the purpose of simplifying the mathematical modelling of the bivariate RVs, we derive some new bivariate QPGWL (BQPGWL) type distributions using the Renyi's copula, Farlie-Gumbel-Morgenstern copula (FGMC), see Morgenstern (1956), Farlie (1960), Gumbel (1960), Gumbel (1961), Johnson (1975) and Johnson (1977) for more details, a modified FGMC that contains four internal types, the Clayton copula (CyC) and Ali-Mikhail-Haq copula (AMHC) (Ali et al., 1987). Based on the Clayton copula, the multivariate QPGWL (MQPGWL) type can be simply formed. Future projects might be devoted to researching these new concepts. For more details, see Pougaza and Djafari (2011), Rodriguez-Lallena and Ubeda-Flores (2004) and Ali et al. (2021a, b). The copulas approaches have been given great attention and efforts in the past few years, for example, see Al-babtain et al. (2020a,b) (for the Clayton copula), Shehata and Yousof (2020, 2021) (for the Farlie-Gumbel-Morgenstern copula and the modified Farlie-Gumbel-Morgenstern copula, among others), Shehata et al. (2020, 2021) (for the Farlie-Gumbel-Morgenstern copula, the Clayton copula, the modified Farlie-Gumbel-Morgenstern copula, and the Renyi's entropy copula), and Elgohari and Yousof (2020b, 2021) (for more details about the Farlie-Gumbel-Morgenstern and modified Farlie-Gumbel-Morgenstern copulas).

Equation (3) is a "concave PDF" if for any $Z_1 \sim \text{QPGWL}(a_1, b_1, \pi_1)$ and $Z_2 \sim \text{QPGWL}(a_2, b_2, \pi_2)$, it satisfies

$$f(\zeta z_1 + \bar{\zeta} z_2) \geq \zeta f_{a_1,b_1,\pi_1}(z_1) + \bar{\zeta} f_{a_2,b_2,\pi_2}(z_2)|_{0 \leq \zeta \leq 1 \text{ and } \bar{\zeta}=1-\zeta}.$$

If the function $f(\zeta z_1 + \bar{\zeta} z_2)$ is twice differentiable, and $f''(\zeta z_1 + \bar{\zeta} z_2) < 0$, $\forall Z \in \mathbb{R}^+$, then $f(\zeta z_1 + \bar{\zeta} z_2)$ is a "strictly convex density function". If $f''(\zeta z_1 + \bar{\zeta} z_2) \leq 0$, $\forall Z \in \mathbb{R}^+$, then $f(\zeta z_1 + \bar{\zeta} z_2)$ is a "convex density function".

Equation (3) is a "convex density function" if for any $Z_1 \sim \text{QPGWL}(a_1, b_1, \pi_1)$ and $X_2 \sim \text{QPGWL}(a_2, b_2, \pi_2)$, the PDF satisfies

$$f(\zeta z_1 + \bar{\zeta} z_2) \leq \zeta f_{a_1,b_1,\pi_1}(z_1) + \bar{\zeta} f_{a_2,b_2,\pi_2}(z_2)|_{0 \leq \zeta \leq 1 \text{ and } \bar{\zeta}=1-\zeta}.$$

If the function $f(\zeta z_1 + \bar{\zeta} z_2)$ is twice differentiable, and $f''(\zeta z_1 + \bar{\zeta} z_2) > 0$, $\forall Z \in \mathbb{R}^+$, then $f(\zeta z_1 + \bar{\zeta} z_2)$ is a "strictly convex density function".

If $f''(\zeta z_1 + \bar{\zeta} z_2) \geq 0$, $\forall Z \in \mathbb{R}^+$, then $f(\zeta z_1 + \bar{\zeta} z_2)$ is a "convex density function". If $f(\zeta z_1 + \bar{\zeta} z_2)$ is a "convex PDF" and ψ is a constant, then the function $\psi f(\zeta z_1 + \bar{\zeta} z_2)$ is a "convex density function". If $f(\zeta z_1 + \bar{\zeta} z_2)$ is a "convex density function", then $[\psi f(\zeta z_1 + \bar{\zeta} z_2)]$ is a convex for every $\psi > 0$. If $f(\zeta z_1 + \bar{\zeta} z_2)$ and $g(\zeta z_1 + \bar{\zeta} z_2)$ are "convex density functions" then $[f(\zeta z_1 + \bar{\zeta} z_2) + g(\zeta z_1 + \bar{\zeta} z_2)]$ is also a "convex density function". If $f(\zeta z_1 + \bar{\zeta} z_2)$ and $g(\zeta z_1 + \bar{\zeta} z_2)$ are "convex density functions", then $[f(\zeta z_1 + \bar{\zeta} z_2). g(\zeta z_1 + \bar{\zeta} z_2)]$ is also a "convex density function". If the function $-f(\zeta z_1 + \bar{\zeta} z_2)$ is a "convex PDF", then the function $f(\zeta z_1 + \bar{\zeta} z_2)$ is a "convex density function". If $f(\zeta z_1 + \bar{\zeta} z_2)$ is a "concave PDF", then $1/f(\zeta z_1 + \bar{\zeta} z_2)$ is a "convex density function" if $f(z) > 0$. If $f(\zeta z_1 + \bar{\zeta} z_2)$ is a "concave density function", $1/f(\zeta z_1 + \bar{\zeta} z_2)$ is a "convex density function" if $f(z) < 0$. If $f(\zeta z_1 + \bar{\zeta} z_2)$ is a "concave density function", $1/f(\zeta z_1 + \bar{\zeta} z_2)$ is a "convex density function".

Since presenting a novel QPGWL model did not become a motivated work itself, is necessary to present some strong motivations and practical justifications that highlight the importance, flexibility and applicability of this distribution. These reasons and drivers essentially developed the new PDF elasticity and the associated HRF. Further, the application ability of the new distribution in modeling and analyzing risks in the field of insurance is one of the most important practical issues for introducing it. Five key risk indicators including the value-at-risk, tail-value-at-risk, tail variance, tail mean-variance, and mean excess loss function are also used to describe the risk exposure associated with the left-skewed insurance claims data. These metrics are created for the QPGWL model. The five primary risk indicators are adopted to assess the left-skewed insurance claim data. Another reason for our motivation to compare

the new distribution's characteristics with those of the left-skewed insurance claims data is the new distribution's wide range of flexibility. The QPGWL model could be useful in modeling in the following cases:

I.   The real data sets whose Kernel density is semi-symmetric and bimodal as shown in Figure 3.
II. The real data sets that have no extreme observations as shown in Figure 6.
III. The asymmetric monotonically increasing hazard rate real data sets as illustrated in Figure 5.

The QPGWL model proved its wide applicability in modeling against common variable Lomax extensions as shown below:

I.   The QPGWL model is evaluated against a number of well-known Lomax extensions, including the exponentiated Lomax extension, the odd log-logistic Lomax extension, the transmuted Topp-Leone Lomax extension, the Kumaraswamy Lomax extension, the Gamma Lomax extension, the special generalized mixture Lomax extension, the Burr Hatke Lomax extension, and the proportional reversed hazard rate Lomax extension, under the consistent-information criteria (CIC), Akaike information criteria (AIC), Bayesian information criteria (BIC) and Hannan-Quinn information criteria (HQIC).
II. The exponentiated Lomax extension, the odd log-logistic Lomax extension, the transmuted Topp-Leone Lomax extension, the Kumaraswamy Lomax extension, the Gamma Lomax extension, the special generalized mixture Lomax extension, the Burr Hatke Lomax extension, and the proportional reversed hazard rate Lomax extension are all compared to the QPGWL model in statistical modelling of the service times of 63 aircraft windshields under the CIC, AIC, BIC and HQIC.
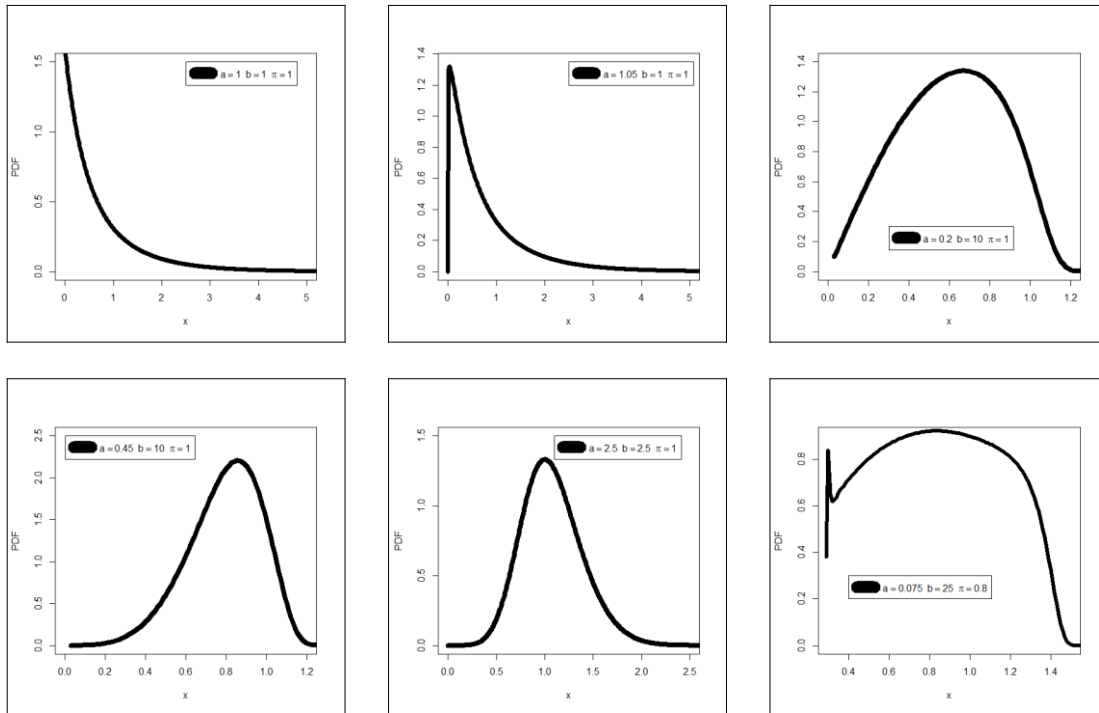
Figure 1: Plots of the QPGWL PDF.
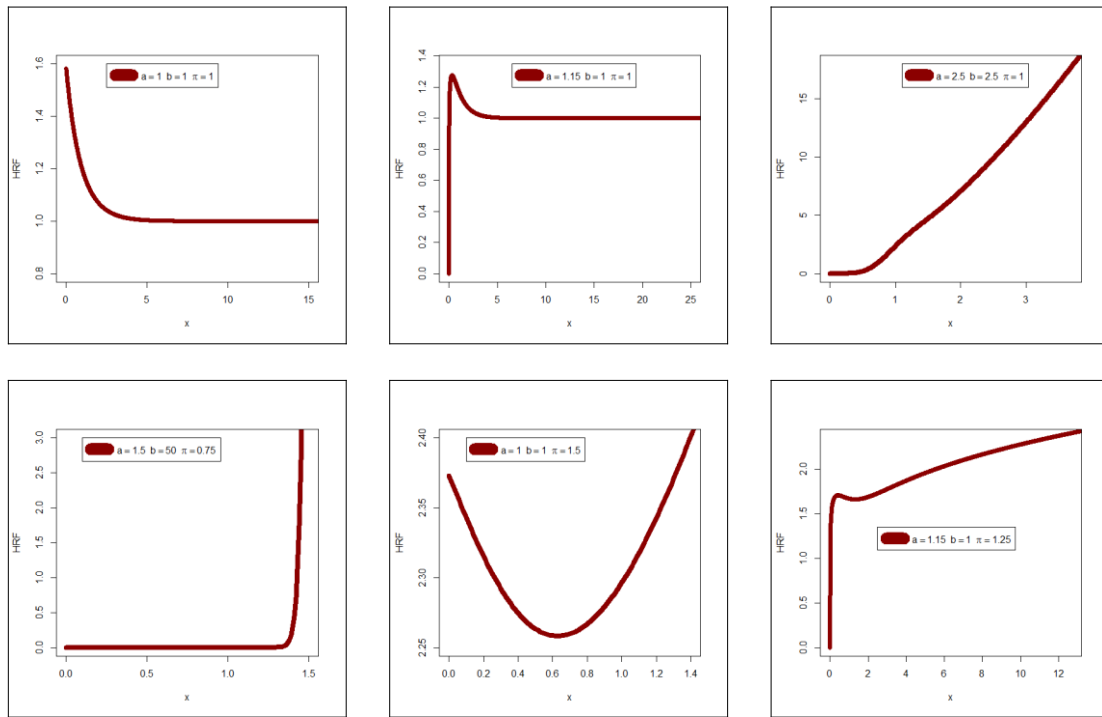
Figure 2: Plots of the QPGWL HRF.

2. Properties
2.1 Expanding the QPGWL density
We create a useful linear representation for the QPGWL density function in this section. The exponentiated Lx (exp-L) model is adopted to express the updated PDF (3). Using the power series, we expand the quantity $A(z)$ as

$$A(z) = exp[-(1 - exp\{-[(1+z)^\pi - 1]^b\})^a] = \sum_{\ell=0}^{\infty} \frac{1}{\ell!}(-1)^\ell \{1 - exp\{-[(1+z)^\pi - 1]^b\}\}^{\ell a}.$$

Then, the PDF (4) can be expressed as

$$f_{a,b,\pi}(z) = \frac{ab\pi}{1 - exp(-1)} \sum_{\ell=0}^{\infty} \frac{(-1)^\ell \, exp\{-[(1+z)^\pi - 1]^b\}}{(1+z)^{1-b\pi}[1 - (1+z)^{-\pi}]^{1-b}} B(z), \tag{5}$$

where

$$B(z) = \{1 - exp\{-[(1+z)^\pi - 1]^b\}\}^{(\ell+1)a - 1}.$$

Then, consider the power series

$$\left(1 - \frac{\varsigma_1}{\varsigma_2}\right)^{\varsigma_3} = \sum_{i=0}^{\infty}(-1)^i \frac{\Gamma(1+\varsigma_3)}{i! \, \Gamma(1-i+\varsigma_3)}\left(\frac{\varsigma_1}{\varsigma_2}\right)^i I_{\left|\frac{\varsigma_1}{\varsigma_2}\right|<1 \text{ and } \varsigma_3>0}. \tag{6}$$

Applying (6) to the quantity $B(z)$ in (5), we can write

$$f_{a,b,\pi}(z) = \frac{ab\pi[1 - (1+z)^{-\pi}]^{b-1}}{[1 - exp(-1)](1+z)^{1-b\pi}} \sum_{\ell,i=0}^{\infty} \frac{(-1)^{\ell+i}\Gamma((\ell+1)a)}{i! \, \ell! \, \Gamma((\ell+1)a - i)} C(z), \tag{7}$$

where

$$C(z) = exp[-(i+1)[(1+z)^\pi - 1]^b]$$

Since

$$(1 + z)^{\pi b - 1} = \frac{(1 + z)^{-\pi - 1}}{[(1 + z)^{-\pi}]^{b+1}}.$$

Then, Equation (7) can be reduced to

$$f_{a,b,\pi}(z) = \frac{ab\pi[1 - (1 + z)^{-\pi}]^{b-1}}{[1 - exp(-1)](1 + z)^{1-b\pi}} \frac{(1 + z)^{-\pi - 1}}{[(1 + z)^{-\pi}]^{b+1}} \sum_{\ell,i=0}^{\infty} \frac{(-1)^{\ell+i} \Gamma((\ell + 1)a)}{i! \, \ell! \, \Gamma((\ell + 1)a - i)} D(z),$$

where

$$D(z) = exp[-(i + 1)[(1 + z)^{\pi} - 1]^{b}].$$

Expanding the quantity $D(z)$ in power series, we can write

$$D(z) = exp\left[-(i + 1)\left[\frac{1 - (1 + z)^{-\pi}}{(1 + z)^{-\pi}}\right]^{b}\right] = \sum_{\wp=0}^{\infty} \frac{(-1)^{\wp}(i + 1)^{\wp}}{\wp!} \frac{[1 - (1 + z)^{-\pi}]^{\wp b}}{[(1 + z)^{-\pi}]^{\wp b}}. \tag{8}$$

Inserting the previous expression of $C(z)$ into the last equation, the QPGWL density has the form

$$f_{a,b,\pi}(z) = \frac{ab\pi(1 + z)^{-\pi - 1}}{1 - exp(-1)} \sum_{\ell,i,\wp=0}^{\infty} (-1)^{\ell+\wp+i} \frac{\Gamma((\ell + 1)a)(i + 1)^{\wp}}{\ell! \, i! \, \wp! \, \Gamma((\ell + 1)a - i)} \frac{[1 - (1 + z)^{-\pi}]^{\wp b + b - 1}}{[(1 + z)^{-\pi}]^{\wp b + b + 1}}. \tag{9}$$

Applying the well-known generalized binomial expansion to $[(1 + z)^{-\pi}]^{(\wp+1)b+1}$, we have

$$[(1 + z)^{-\pi}]^{(\wp+1)b+1} = \sum_{q=0}^{\infty} \frac{\Gamma(b^{\star} + 1)[1 - (1 + z)^{-\pi}]^{q}}{q! \, \Gamma(\wp b + b + 1)} \Big|_{b^{\star}=(\wp+1)b+q}. \tag{10}$$

By inserting (10) into Equation (9), the QPGWL density reduces to

$$f_{a,b,\pi}(z) = \sum_{\wp,q=0}^{\infty} \zeta_{\wp,q} \, \hbar_{b^{\star}}(z), \tag{11}$$

where

$$\hbar_{b^{\star}}(z) = b^{\star}\pi(1 + z)^{-\pi - 1}[1 - (1 + z)^{-\pi}]^{b^{\star} - 1}$$

is the exponentiated-L (exp-L) PDF with power parameter $b^{\star}$ and

$$\zeta_{\wp,q} = \sum_{\ell,i=0}^{\infty} \frac{ab}{[1 - exp(-1)]} \frac{(-1)^{\ell+\wp+i}(i + 1)^{\wp} \Gamma([l + 1]a)\Gamma([\wp + 1]b + q + 1)}{\ell! \, i! \, \wp! \, q! \, \Gamma([l + 1]a - i)\Gamma([\wp + 1]b + 1)b^{\star}}.$$

Equation (11) reveals that the PDF of the QPGWL model can be written as a linear combination of exp-L densities. Then, based on the characteristics of the exp-L distribution, one can obtain those of the QPGWL model. Similarly, the CDF of the QPGWL distribution can also be expressed as a linear combination of exp-L CDFs

$$F_{a,b,\pi}(z) = \sum_{\wp,q=0}^{\infty} \zeta_{\wp,q} \, \mathbf{H}_{b^{\star}}(z), \tag{12}$$

where $\mathbf{H}_{b^{\star}}(z)$ is the exp-L CDF with power parameter $b^{\star}$.

2.2 Moments
The calculations below involve several special functions, including the complete beta function

$$B(\varsigma_1, \varsigma_2) = \int_0^1 x^{\varsigma_1 - 1} (1 - x)^{\varsigma_2 - 1} dx,$$

the incomplete beta function

$$B_{\varsigma_3}(\varsigma_1, \varsigma_2) = \int_0^{\varsigma_3} x^{\varsigma_1 - 1} (1 - x)^{\varsigma_2 - 1} dx,$$

the complete gamma function

$$\boldsymbol{\Gamma}(1 + \varsigma_1) = \varsigma_1! = \prod_{\varsigma_2=0}^{\varsigma_1 - 1} (\varsigma_1 - \varsigma_2) = \int_0^{+\infty} x^{\varsigma_1} exp(-x) \, dx.$$

the lower incomplete gamma function

$$\gamma(\varsigma_1, \varsigma_2) = \int_0^{\varsigma_2} y^{\varsigma_1 - 1} \, exp(-y) \, dy = \sum_{\varsigma_3 = 0}^{+\infty} \frac{(-1)^{\varsigma_3} \varsigma_2^{\varsigma_1 + \varsigma_3}}{\Gamma(1 + \varsigma_3)(\varsigma_1 + \varsigma_3)},$$

and the upper incomplete gamma function, where

$$\mathbf{\Gamma}(\varsigma_1) = \mathbf{\Gamma}(\varsigma_1, \varsigma_2) + \gamma(\varsigma_1, \varsigma_2).$$

Let $Y_{b^\star}$ be a RV having the exp-L family with power $b^\star > 0$ defined in (11) and Z be a RV having the QPGWL(a, b, π) model. Then, the rth moment of the RV Z is

$$\mu'_{r,Z} = \mathbb{E}(Z^r) = \sum_{p,q=0}^{\infty} \sum_{\varsigma=0}^{r} \zeta_{p,q} \, b^\star (-1)^\varsigma \binom{r}{\varsigma} B\left(b^\star, 1 + \frac{\varsigma - r}{\pi}\right)|_{\pi > r}. \qquad (13)$$

2.3 Moment generating function (MGF)

Clearly, the MGF can be derived from Equation (10) as

$$M_Z(t) = \sum_{p,q,r=0}^{\infty} \sum_{\varsigma=0}^{r} \frac{t^r}{r!} \zeta_{p,q} b^\star (-1)^\varsigma \binom{r}{\varsigma} B\left(b^\star, 1 + \frac{\varsigma - r}{\pi}\right)|_{\pi > r}.$$

2.4 Incomplete moments

The rth incomplete moment, say $\boldsymbol{\delta}_{r,Z}(t)$, of the RV Z can be obtained from (10) as

$$\boldsymbol{\delta}_{r,Z}(t) = \sum_{p,q=0}^{n} \zeta_{p,q} \, \boldsymbol{\delta}_{r,b^\star}^{-\infty,t}(t),$$

where

$$\boldsymbol{\delta}_{r,b^\star}^{-\infty,t}(t) = \int_{-\infty}^{t} z^r \, \boldsymbol{\hbar}_{b^\star}(z) dz.$$

Then, the rth incomplete moment has the form

$$\boldsymbol{\delta}_{r,Z}(t) = \sum_{p,q=0}^{\infty} \sum_{\varsigma=0}^{r} \zeta_{p,q} \, b^\star (-1)^\varsigma \binom{r}{\varsigma} B_t\left(b^\star, 1 + \frac{\varsigma - r}{\pi}\right)|_{\pi > r},$$

and the 1$^{\text{st}}$ incomplete moment becomes

$$\boldsymbol{\delta}_{1,Z}(t) = \sum_{p,q=0}^{+\infty} \sum_{\varsigma=0}^{r} \zeta_{p,q} \, b^\star (-1)^\varsigma \binom{1}{\varsigma} B_t\left(b^\star, 1 + \frac{\varsigma - 1}{\pi}\right)|\pi > 1.$$

The mean deviations (MDs) of the RV Z about the $\mu'_{1,Z}$ are $\mathbb{E}(|Z - \mu'_{1,Z}|) = \mathcal{M}_1(\mu'_{1,Z})$ and the MDs about the median (D) are $\mathbb{E}(|Z - D|) = \mathcal{M}_{2,Z}(D)$. They can be given by $\mathcal{M}_{1,Z}(\mu'_{1,Z}) = 2\mu'_{1,Z}F(\mu'_{1,Z}) - 2\boldsymbol{\delta}_{1,Z}(\mu'_{1,Z})$ and $\mathcal{M}_{2,Z}(D) = \mu'_{1,Z} - 2\boldsymbol{\delta}_{1,Z}(D)$, respectively, where $\mu'_{1,Z} = \mathbb{E}(Z)$, $D = Q\left(\frac{1}{2}\right)$ is the median of Z and $\boldsymbol{\delta}_{1,Z}(t)$ is given above. These results for $\boldsymbol{\delta}_{1,Z}(t)$ can be applied for constructing the Bonferroni ($\mathcal{B}on(\mathcal{D})$) and Lorenz ($Lor(\mathcal{D})$) curves defined (for a probability $\mathcal{D}$) by $\mathcal{B}on(\mathcal{D}) = \boldsymbol{\delta}_{1,Z}(Q(\mathcal{D}))/(\mathcal{D}\mu'_{1,Z})$ and $Lor(\mathcal{D}) = \boldsymbol{\delta}_{1,Z}(Q(\mathcal{D}))/\mu'_{1,Z}$, respectively.

2.5 Residual life (RL) and reversed residual life (RRL)

The jth moment of the RL of the RV Z can be obtained from $w_{j,Z}(t) = \mathbb{E}[(Z - t)^j]|_{Z > t \text{ and } j \in \mathbb{N}}$ or from

$$w_{j,Z}(t) = \frac{1}{1 - F_{a,b,\pi}(t)} \int_t^\infty (z - t)^j f_{a,b,\pi}(z) dz,$$

which can also be written as

$$w_{j,Z}(t) = \frac{1}{1 - F_{a,b,\pi}(t)} \sum_{p,q=0}^{\infty} \sum_{m=0}^{j} \zeta_{p,q} \binom{j}{m} (-t)^{j-m} \boldsymbol{\delta}_{j,b^\star}^{t,+\infty}(t).$$

Then,

$$w_{j,Z}(t) = \frac{1}{1 - F_{a,b,\pi}(t)} \sum_{p,q=0}^{\infty} \sum_{\varsigma=0}^{j} \zeta_{p,q,\varsigma}(w,j)\, b^{\star}(-1)^{\varsigma} \binom{j}{\varsigma} B_t\left(b^{\star}, 1 + \frac{\varsigma - j}{\pi}\right)\Big|_{t>0, j\in\mathbb{N}, \pi>j},$$

where

$$\boldsymbol{\zeta}_{p,q,\varsigma}(w,j) = \boldsymbol{\zeta}_{p,q} \sum_{m=0}^{j} \binom{j}{m}(-t)^{j-m}.$$

For $j = 1$, we obtain the mean of the residual life (MRL) which can follow from $w_{1,Z}(t) = \mathbb{E}[(Z - t)]|_{Z>t \ and \ j\in\mathbb{N}}$ as

$$w_{1,Z}(t) = \frac{1}{1 - F_{a,b,\pi}(t)} \sum_{p,q=0}^{+\infty} \sum_{\varsigma=0}^{1} \zeta_{p,q,\varsigma}(w,1)\, b^{\star}(-1)^{\varsigma} \binom{1}{\varsigma} B_t\left(b^{\star}, 1 + \frac{\varsigma - 1}{\pi}\right)\Big|_{t>0, j=1, \pi>j},$$

where

$$\boldsymbol{\zeta}_{p,q,\varsigma}(w,1) = \boldsymbol{\zeta}_{p,q} \sum_{m=0}^{1} \binom{1}{m}(-t)^{1-m}.$$

On the other hand, the jth moment of the RRL is $\boldsymbol{W}_{j,Z}(t) = \mathbb{E}[(t - Z)^j]|_{Z\leq t, t>0 \ and \ j\in\mathbb{N}}$ or

$$\boldsymbol{W}_{j,Z}(t) = \frac{1}{F_{a,b,\pi}(t)} \int_0^t (t - z)^j f_{a,b,\pi}(z)dz,$$

which can also be expressed as

$$\boldsymbol{W}_{j,Z}(t) = \frac{1}{F_{a,b,\pi}(t)} \sum_{\boldsymbol{p,q}=0}^{\infty} \sum_{m=0}^{j} \boldsymbol{\zeta}_{\boldsymbol{p,q}}(-1)^m \binom{j}{m} t^{j-m} \boldsymbol{\delta}_{j,b^{\star}}^{-\infty,t}(t).$$

Hence,

$$\boldsymbol{W}_{j,Z}(t) = \frac{1}{F_{\underline{V}}(t)} \sum_{p,q=0}^{+\infty} \sum_{\varsigma=0}^{j} \boldsymbol{\zeta}_{p,q,\varsigma}(\boldsymbol{W},j)\, b^{\star}(-1)^{\varsigma} \binom{j}{\varsigma} B_t\left(b^{\star}, 1 + \frac{\varsigma - j}{\pi}\right)\Big|_{t>0, j\in\mathbb{N}, \pi>j},$$

where

$$\boldsymbol{\zeta}_{p,q,\varsigma}(\boldsymbol{W},j) = \boldsymbol{\zeta}_{p,q} \sum_{m=0}^{j} (-1)^m \binom{j}{m} t^{j-m}.$$

For $j = 1$, we obtain the mean waiting time (MWT), also called the mean inactivity time (MIT), which can be derived from $\boldsymbol{W}_{1,Z}(t) = \mathbb{E}[(t - Z)]|_{Z\leq t, t>0 \ and \ j=1}$ as

$$\boldsymbol{W}_{1,Z}(t) = \frac{1}{F_{a,b,\pi}(t)} \sum_{p,q=0}^{\infty} \sum_{\varsigma=0}^{1} \boldsymbol{\zeta}_{p,q,\varsigma}(\boldsymbol{W},1)\, b^{\star}(-1)^{\varsigma} \binom{1}{\varsigma} B_t\left(b^{\star}, 1 + \frac{\varsigma - 1}{\pi}\right)\Big|_{t>0, j=1, \pi>j},$$

where

$$\boldsymbol{\zeta}_{p,q,\varsigma}(\boldsymbol{W},1) = \boldsymbol{\zeta}_{p,q} \sum_{m=0}^{1} (-1)^m \binom{1}{m} t^{1-m}.$$

3. Copula
3.1 BQPGWL type via CyC
Consider that $X_1 \sim \text{QPGWL}(a_1, b_1, \pi_1)$ and $X_2 \sim \text{QPGWL}(a_2, b_2, \pi_2)$. The CyC depending on the continuous marginal functions $\overline{Z} = 1 - Z$ and $\overline{Y} = 1 - Y$ can be expressed as

$$C_\zeta(\overline{Z}, \overline{Y}) = \left[\max\left(\overline{Z}^{-\zeta} + \overline{Y}^{-\zeta} - 1\right); 0\right]^{-\frac{1}{\zeta}}, \zeta \in [-1, \infty) - \{0\}, \overline{Z} \in (0,1) \ and \ \overline{Y} \in (0,1). \quad (14)$$

Let $\overline{Z} = 1 - F_{a_1,b_1,\pi_1}(z_1)|_{a_1,b_1,\pi_1}$, $\overline{Y} = 1 - F_{a_2,b_2,\pi_2}(z_2)|_{a_2,b_2,\pi_2}$. Then, the BQPGWL type distribution can be obtained from (14). A straightforward multivariate QPGWL (m-dimensional extension) via CyC can be easily determined analogously. The m-dimensional extension via CyC which is a function operating in $[0,1]^m$, and in that case, z_i is not a value in $[0,1]$ necessarily.

3.2 BQPGWL type via Renyi's copula

The Renyi's copula can defined as $C(\mathcal{Z}, \mathcal{Y}) = z_2 \mathcal{Z} + z_1 \mathcal{Y} - z_1 z_2$, where the continuous marginal functions $\mathcal{Z} = 1 - \overline{\mathcal{Z}} = F_{V_1}(z_1) \in (0,1)$ and $\mathcal{Y} = 1 - \overline{\mathcal{Y}} = F_{V_1}(z_2) \in (0,1)$, and the values z_1 and z_2 are chosen to guarantee that $C(\mathcal{Z}, \mathcal{Y})$ is a copula. Then, the associated CDF of the BQPGWL has the form

$$F(z_1, z_2) = C\left(F_{a_1,b_1,\pi_1}(z_1), F_{a_2,b_2,\pi_2}(z_2)\right),$$

where $F_{a_1,b_1,\pi_1}(z_1)$ and $F_{a_2,b_2,\pi_2}(z_2)$ are defined above. It is worth mentioning that, in [18] the authors emphasized that this copula does not show a closed shape and numerical approaches become necessary.

3.3 BQPGWL type via FGMC

Considering the FGMC, the joint CDF has the form

$$C_\zeta(\mathcal{Z}, \mathcal{Y}) = \mathcal{Z}\mathcal{Y}(1 + \zeta \overline{\mathcal{Z}}\, \overline{\mathcal{Y}}),$$

where the continuous marginal function $\mathcal{Z} \in (0,1)$, $\mathcal{Y} \in (0,1)$, $\zeta \in [-1,1]$ and $C_\zeta(\mathcal{Z}, 0) = C_\zeta(0, \mathcal{Y}) = 0|_{(\mathcal{Z},\mathcal{Y} \in (0,1))}$, which is a "grounded minimum condition " and $C_\zeta(\mathcal{Z}, 1) = \mathcal{Z}$ and $C_\zeta(1, \mathcal{Y}) = \mathcal{Y}$, which is a "grounded maximum condition ". The grounded minimum/maximum conditions are valid for any copula. Setting $\overline{\mathcal{Z}} = \overline{\mathcal{Z}}_{V_1}|_{V_1 > 0}$ and $\overline{\mathcal{Y}} = \overline{\mathcal{Y}}_{V_2}|_{V_2 > 0}$, we have

$$F(z_1, z_2) = C\left(F_{a_1,b_1,\pi_1}(z_1), F_{a_2,b_2,\pi_2}(z_2)\right) = \mathcal{Z}\mathcal{Y}(1 + \zeta \overline{\mathcal{Z}}\, \overline{\mathcal{Y}}).$$

The joint PDF reduces to

$$c_\zeta(\mathcal{Z}, \mathcal{Y}) = 1 + \zeta \mathcal{Z}^\star \mathcal{Y}^\star, (\mathcal{Z}^\star = 1 - 2\mathcal{Z} \text{ and } \mathcal{Y}^\star = 1 - 2\mathcal{Y})$$

or from

$$f_\zeta(z_1, z_2) = f_{a_1,b_1,\pi_1}(z_1) f_{a_2,b_2,\pi_2}(z_2) c\left(F_{a_1,b_1,\pi_1}(z_1), F_{a_2,b_2,\pi_2}(z_2)\right),$$

where the two functiona $c_\zeta(\mathcal{Z}, \mathcal{Y})$ and $f_\zeta(z_1, z_2)$ are densities corresponding to the joint CDFs $C_\zeta(\mathcal{Z}, \mathcal{Y})$ and $F_\zeta(z_1, z_2)$.

3.4 BQPGWL type via modified FGMC

The formula of the modified FGMC can written as

$$C_\zeta(\mathcal{Z}, \mathcal{Y}) = \mathcal{Z}\mathcal{Y} + \zeta \mathcal{O}(\mathcal{Z})^\bullet \mathcal{H}(\mathcal{Y})^\bullet,$$

where $\mathcal{O}(\mathcal{Z})^\bullet = \mathcal{Z}\overline{\mathcal{O}(\mathcal{Z})}$ and $\mathcal{H}(\mathcal{Y})^\bullet = \mathcal{Y}\overline{\mathcal{H}(\mathcal{Y})}$, $\mathcal{O}(\mathcal{Z}) \in (0,1)$ and $\mathcal{H}(\mathcal{Y}) \in (0,1)$ are two continuous functions such that $\mathcal{O}(\mathcal{Z} = 0) = \mathcal{O}(\mathcal{Z} = 1) = \mathcal{H}(\mathcal{Y} = 0) = \mathcal{H}(\mathcal{Y} = 1) = 0$. Let

$$\alpha[\mathcal{O}(\mathcal{Z})^\bullet] = inf\left\{\mathcal{O}(\mathcal{Z})^\bullet : \frac{\partial}{\partial \mathcal{Z}}\mathcal{O}(\mathcal{Z})^\bullet, \forall \Delta_1(\mathcal{Z})\right\} < 0,$$

$$\xi[\mathcal{H}(\mathcal{Y})^\bullet] = inf\left\{\mathcal{H}(\mathcal{Y})^\bullet : \frac{\partial}{\partial \mathcal{Y}}\mathcal{H}(\mathcal{Y})^\bullet, \forall \Delta_2(\mathcal{Y})\right\} > 0,$$

$$\beta[\mathcal{O}(\mathcal{Z})^\bullet] = sur\left\{\mathcal{O}(\mathcal{Z})^\bullet : \frac{\partial}{\partial \mathcal{Z}}\mathcal{O}(\mathcal{Z})^\bullet, \forall \Delta_1(\mathcal{Z})\right\} < 0,$$

$$\eta[\mathcal{H}(\mathcal{Y})^\bullet] = sur\left\{\mathcal{H}(\mathcal{Y})^\bullet : \frac{\partial}{\partial \mathcal{Y}}\mathcal{H}(\mathcal{Y})^\bullet, \forall \Delta_2(\mathcal{Y})\right\} > 0.$$

Then for

$$1 \leq min(\beta[\mathcal{O}(\mathcal{Z})^\bullet]\alpha[\mathcal{O}(\mathcal{Z})^\bullet], \eta[\mathcal{H}(\mathcal{Y})^\bullet]\xi[\mathcal{H}(\mathcal{Y})^\bullet]) < \infty$$

we have

$$0 = \frac{\partial}{\partial \mathcal{Z}}\mathcal{O}(\mathcal{Z})^\bullet - \frac{z}{\partial \mathcal{Z}}\partial\mathcal{O}(\mathcal{Z}) - \mathcal{O}(\mathcal{Z}),$$

where

$$\Delta_1(\mathcal{Z}) = \frac{\partial}{\partial \mathcal{Z}} \mathcal{O}(\mathcal{Z})^{\bullet} \text{ exists,}$$

and

$$\Delta_2(\mathcal{Y}) = \frac{\partial}{\partial \mathcal{Y}} \mathcal{H}(\mathcal{Y})^{\bullet} \text{ exists.}$$

The following four types can be determined:
● *Modified FGMC Type I*
Consider $\mathcal{O}(\mathcal{Z})^{\bullet} = \mathcal{Z}\overline{\mathcal{O}(\mathcal{Z})}$ and $\mathcal{H}(\mathcal{Y})^{\bullet} = \mathcal{Y}\overline{\mathcal{H}(\mathcal{Y})}$, where $\mathcal{O}(\mathcal{Z}) \in (0,1)$ and $\mathcal{H}(\mathcal{Y}) \in (0,1)$ are two continuous functions, and $\mathcal{O}(\mathcal{Z} = 0) = \mathcal{O}(\mathcal{Z} = 1) = \mathcal{H}(\mathcal{Y} = 0) = \mathcal{H}(\mathcal{Y} = 1) = 0$ satisfy the above conditions. Then, the new bivariate version via modified FGMC type I can be obtained from

$$C_\zeta(\mathcal{Z}, \mathcal{Y}) = \mathcal{Z}\mathcal{Y} + \zeta \mathcal{O}(\mathcal{Z})^{\bullet} \mathcal{H}(\mathcal{Y})^{\bullet}.$$

● *Modified FGMC Type II*
Consider $A(\mathcal{Z}; \zeta_1)$ and $B(\mathcal{Y}; \zeta_2)$ that satisfy the above conditions, where $A(\mathcal{Z}; \zeta_1)|_{(\zeta_1 > 0)} = \mathcal{Z}^{\zeta_1}(1 - \mathcal{Z})^{1-\zeta_1}$ and $B(\mathcal{Y}; \zeta_2)|_{(\zeta_2 > 0)} = \mathcal{Y}^{\zeta_2}(1 - \mathcal{Y})^{1-\zeta_2}$. Then, the corresponding bivariate version (modified FGMC **Type II**) can be obtained from

$$C_{\zeta_0, \zeta_1, \zeta_2}(\mathcal{Z}, \mathcal{Y}) = \mathcal{Z}\mathcal{Y}[1 + \zeta_0 A(\mathcal{Z}; \zeta_1)B(\mathcal{Y}; \zeta_2)].$$

● *Modified FGMC Type III*
Let $\widetilde{A(\mathcal{Z})} = \mathcal{Z}[\varsigma og(1 + \overline{\mathcal{Z}})]|_{(\overline{\mathcal{Z}} = 1 - \mathcal{Z})}$ and $\widetilde{B(\mathcal{Y})} = \mathcal{Y}[\varsigma og(1 + \overline{\mathcal{Y}})]|_{(\overline{y} = 1 - y)}$. Then, the associated CDF of the BQPGWL-FGM (modified FGMC type **III**) is

$$C_\zeta(\mathcal{Z}, \mathcal{Y}) = \mathcal{Z}\mathcal{Y}[1 + \zeta \widetilde{A(\mathcal{Z})} \widetilde{B(\mathcal{Y})}].$$

● *Modified FGMC Type IV*
Using the quantile concept, the CDF of the BQPGWL-FGM (modified FGMC type **IV**) model can be obtained from

$$C(\mathcal{Z}, \mathcal{Y}) = \mathcal{Z}F^{-1}(\mathcal{Z}) - F^{-1}(\mathcal{Z})F^{-1}(\mathcal{Y}) + \mathcal{Y}F^{-1}(\mathcal{Y})$$

where $F^{-1}(\mathcal{Z}) = Q(\mathcal{Z})$ and $F^{-1}(\mathcal{Y}) = Q(\mathcal{Y})$.

3.5 BQPGWL type via AMHC
Under the "stronger Lipschitz condition" and following Ali et al. (1978), the joint CDF of the Archimedean *AMHC* can be expressed as

$$C_\zeta(\mathcal{Z}, \mathcal{Y}) = \frac{\mathcal{Z}\mathcal{Y}}{1 - \zeta \overline{\mathcal{Z}\mathcal{Y}}} |_{\zeta \in (-1,1)},$$

and the corresponding joint PDF of the Archimedean *AMHC* reduces to

$$c_\zeta(\mathcal{Z}, \mathcal{Y}) = \frac{1}{[1 - \zeta \overline{\mathcal{Z}\mathcal{Y}}]^2}\left(1 - \zeta + 2\zeta \frac{\mathcal{Z}\mathcal{Y}}{1 - \zeta \overline{\mathcal{Z}\mathcal{Y}}}\right)|_{\zeta \in (-1,1)}.$$

Then, for any $\overline{\mathcal{Z}} = 1 - F_{a_1, b_1, \pi_1}(z_1) = |_{[\overline{\mathcal{Z}} = (1-\mathcal{Z}) \in (0,1)]}$ and $\overline{\mathcal{Y}} = 1 - F_{a_2, b_2, \pi_2}(z_2)|_{[\overline{y} = (1-y) \in (0,1)]}$, we have

$$C_\zeta(z_1, z_2) = \frac{F_{a_1, b_1, \pi_1}(z_1)F_{a_2, b_2, \pi_2}(z_2)}{1 - \zeta[1 - F_{\underline{V}_1}(z_1)][1 - F_{a_2, b_2, \pi_2}(z_2)]} |_{\zeta \in (-1,1)}$$

and

$$c_\zeta(z_1, z_2) = \frac{1 - \zeta + 2\zeta\left\{\dfrac{F_{a_1, b_1, \pi_1}(z_1)F_{a_2, b_2, \pi_2}(z_2)}{1 - \zeta[1 - F_{a_1, b_1, \pi_1}(z_1)][1 - F_{a_2, b_2, \pi_2}(z_2)]}\right\}}{\left\{1 - \zeta[1 - F_{a_1, b_1, \pi_1}(z_1)][1 - F_{a_2, b_2, \pi_2}(z_2)]\right\}^2} |_{\zeta \in (-1,1)}.$$

4. The key risk indicators
Probability-based distributions may provide an adequate explanation of risk exposure. The degree of risk exposure is typically expressed as one number, or at the very least a small set of numbers. These risk exposure levels, which are usually referred to as key risk indicators (KRIs), are obviously functions of a particular model. Such KRIs give actuaries and risk managers knowledge about the level of a company's exposure to particular risks. There are many KRIs that can be considered and researched, including value-at-risk (VaR), tail-value-at-risk (TVaR), conditional-value-at-risk (CVaR), tail variance (TV), and tail Mean-Variance (TMV), among others. A quantile of the distribution

of total losses in particular is the VaR. The VaR indicator can be used to indicate the chance of a bad outcome at a particular probability/confidence level. Actuaries and risk managers usually concentrate on this task.

The risk exposure under insurance claims data was also described using five important risk indicators, including value-at-risk, tail-value-at-risk, tail variance, tail mean-variance, and mean excess loss function. These metrics are developed for the proposed weighted exponential model. In accordance with the five separate risk indicators, the insurance claims data are employed in the risk analysis. We chose to focus on examining the insurance claims data under the five primary risk indicators since it has a straightforward tail to the left and only one peak. We were inspired to provide both a numerical and graphical risk assessment and analysis because the new distribution was flexible enough to model the insurance claims data under some risk indicators. By matching the new distribution's characteristics to those of the insurance claims data, we were further motivated.

4.1 VaR indicator

Risk exposure is an inevitable occurrence for any insurance organization. As a result, actuaries created a variety of risk indicators to assess how much a collection of assets might lose. One of the widely used benchmark risk indicators to assess risk exposure is now represented by this indicator numerically. The VaR indicator measures the risk of a prospective loss for the insurance company and calculates how likely a loss is given a certain likelihood. In general, the VaR estimates the amount of capital necessary to guarantee that the business does not officially go insolvent with a specific likelihood.

The level of assurance picked is arbitrary. Therefore, many VaR values may be taken into account for various levels of confidence. It can be a high percentage, like 99.95 percent for the entire company, or it can be a low percentage, like 95 percent, for just one unit or risk class within the insurance company. These various percentages can represent the inter-unit or inter-risk type diversification that exists.

Definition 1: *Let Z denote a loss RV. Then, the VaR of Z at the $100q\%$ level, say VaRq $(Z; \eta, \psi)$ or $\pi(q)$, is the $100q\%$ quantile (or percentile) of the distribution of Z .*
Then, based on Definition 1, we can simply write for the QPGWL distribution.

$$Pr(Z > Q_U) = \begin{cases} 1\%|_{q=99\%} \\ 5\%|_{q=95\%} \\ \vdots \end{cases},$$

where Q_U is the quantile function. For a one-year time when $= 99.5\%$, the interpretation is that there is only a very small chance (0.5%) that the insurance company will be bankrupted by an adverse outcome over the next year. The quantity VaR $(Z; \eta, \psi)$ does not satisfy one of the four criteria for coherence (Wirch, 1999).

4.2 TVaR risk indicator

The VaR indicator is widely utilized in the management of financial risk over a specified relatively brief time period as a risk assessment. In these situations, both gains and losses are frequently described using the normal distribution. If the distribution of gains (or losses) is limited to the normal distribution, the quantity VaRq(Z) meets all coherence conditions. The data sets for insurance claims, however, are frequently distorted. Using the normal distribution to describe insurance claims is the next step.

Definition 2: *Let Z denote a loss RV. The TVaRq of Z at the $100q\%$ confidence level is the expected loss given that the loss exceeds the $100q\%$ of the distribution of Z,* namely

$$\text{TVaRq}(Z; a, b, \pi) = E(Z|Z > \pi(q)) = \frac{1}{1 - F_{a,b,\pi}(\pi(q))} \int_{\pi(q)}^{\infty} z f_{\underline{V}}(z) dx = \frac{1}{1-q} \int_{\pi(q)}^{\infty} z f_{a,b,\pi}(z) dx.$$

Thus, the quantity TVaRq $(Z; a, b, \pi)$ is an average of all VaR values above at the confidence level q, which provides more information about the tail of the QPGWL distribution. Further, it can be reduced to

$$\text{TVaRq}(Z; a, b, \pi) = \text{VaRq}(Z; a, b, \pi) + l(\text{VaRq}(Z; a, b, \pi)),$$

where $l\big(\text{VaRq}(Z; a, b, \pi)\big)$ is the mean excess loss function evaluated at the $100q\%$ th quantile. So, TVaRq $(Z; \eta, \psi)$ is larger than its corresponding VaRq $(Z; a, b, \pi)$ by the amount of average excess of all losses that exceed the ELq$(Z; a, b, \pi)$ value of VaRq $(Z; a, b, \pi)$. In the insurance literature, TVaRq $(Z; a, b, \pi)$ has been developed independently and it is also called the conditional tail expectation (Wirch,1999). It has also been called the tail conditional expectation (TCE) or expected shortfall (ES) (Tasche, 2002; Acerbi and Tasche, 2002).

4.3 TV risk indicator

The TV risk indicator, which Furman and Landsman (2006) established, calculates the loss's deviation from the average along a tail. Explicit formulas for the TV risk indicator under the multivariate normal distribution were also developed by Furman and Landsman (2006).

Definition 3: Let Z denote *a loss RV. The TV risk indicator, say TVq(Z), is*
$$\text{TVq}(Z; a, b, \pi) = E\big(Z^2 | Z > \pi(q)\big) - [\text{TVaRq}(Z; a, b, \pi)]^2.$$

4.4 TMV risk indicator

As a metric for the best portfolio choice, Landsman (2010) developed the TMV risk indicator based on the TCE risk indicator and the TV risk indicator.

Definition 3: Let Z denote *loss RV. The TMV risk indicator can be expressed as*

$$\text{TMVq}(Z; a, b, \pi, \varsigma) = \text{TVaRq}(Z; a, b, \pi) + \varsigma \text{TVq}(Z; a, b, \pi)|_{0<\varsigma<1}.$$

Then, for any LRV, TMVq$(Z; a, b, \pi, \varsigma) > $ TVq $(Z; a, b, \pi)$ and, for $\varsigma = 0$, TMVq$(Z; a, b, \pi) = $ TVaRq$(Z; a, b, \pi)$.

5. The maximum likelihood method

The maximum likelihood method is a statistical technique for estimating the parameters of a probability distribution that has been assumed given some observed data. This is accomplished by maximizing a likelihood function to make the observed data as probable as possible given the assumed statistical model. The maximum likelihood estimate is the location in the parameter space where the likelihood function is maximized. Maximum likelihood is a popular approach for making statistical inferences since its rationale is clear and adaptable. The derivative test for figuring out maxima can be used if the likelihood function is differentiable. The ordinary least squares estimator, for example, maximizes the likelihood of the linear regression model, allowing the first-order requirements of the likelihood function to be explicitly solved in some circumstances. However, in the majority of cases, it will be essential to use numerical techniques to determine the probability function's maximum.

We represent a collection of data as a random sample drawn from a joint probability distribution that is unknown and described in terms of a number of factors. Finding the parameters for which the observed data have the highest joint probability is the aim of maximum likelihood estimation. Let $Z_1, \dots, Z_n$ be any observed random sample (RS) from the QPGWL model. Then, the log-likelihood function ($\ell_{a,b,\pi}$) can be derived from

$$\ell_{a,b,\pi} = \log\left[\prod_{i=1}^{n} f_{a,b,\pi}(z_i)\right]$$

and can then be maximized directly using many common packages such as the R software ("optim function") or, in some cases, by solving the system of the nonlinear equations of the likelihood derivations from the differentiating $\ell_{a,b,\pi}$ with respect to a, b, π. The score vector components

$$\mathbf{U}_a = \frac{\partial}{\partial a} \ell_{a,b,\pi}, \mathbf{U}_b = \frac{\partial}{\partial b} \ell_{a,b,\pi} \text{ and } \mathbf{U}_\pi = \frac{\partial}{\partial \pi} \ell_{a,b,\pi}$$

can be derived to obtain the nonlinear system $\mathbf{U}_a = \mathbf{U}_b = \mathbf{U}_\pi = 0$ and then solving them simultaneously to find the maximum likelihood estimates (MLEs) of a, b, π. This system can only be solved numerically for the complicated models using some common iterative algorithms such as the "Newton-Raphson" algorithms. The qualities of consistency and asymptotic normalcy are satisfied under regularity criteria, as usual. The asymptotic distribution, in particular, is multivariate normal behind the MLEs. To construct confidence intervals (CIs), confidence regions, and various likelihood tests, we can use first-order asymptotic theory.

6. Applications

In this section, we examine two actual data sets in an effort to limit the new QPGWL model's widespread applicability. The Quantile-Quantile (Q-Q) plots, Total Time in Test (TTT) plots, Non-parametric Kernel Density Estimation (NKDE) plots, and Box Plots are just a few examples of valuable graphical tools that are employed.

The first data set called the aircraft windshield data and represented failure times of 84 aircraft windshield. The second data set also called the aircraft windshield but represents service times of 63 aircraft windshield. Murthy et al. (2004) gave the two actual data. You can find numerous additional helpful symmetric and asymmetric data sets in Aryal et al. (2017), Yousof et al. (2016, 2018a), and Altun et al. (2018a, b). Here, we refer to Merovci et al. (2017), Hamedani et al. (2017, 2018, 2019), Aryal and Yousof (2017), Nascimento et al. (2019), Alizadeh et al. (2018, 2020a,b), Merovci et al. (2020), Karamikabir et al. (2020), Korkmaz et al. (2018a,b, 2020), Elgohari et al. (2021), and Almazah et al. (2021) to find other related applications to real-life data sets. The basic PDF shape is explored using the NKDE tool (see Figure 3). The Q-Q plot is used to determine whether the two real data sets are "normal" (see Figure 4). The TTT tool is adopted to examine the basic HRFs shape (Figure 5). The "box plot" verifies the outliers (Figure 6).

It can be seen from left panel of Figure 3 that the first data's NKDE is left-skewed with bimodal shape. The right panel of Figure 3 proves that the second data's NKDE is also left-skewed with bimodal shape. The left and right panels of Figures 4 show that there is a "normality" for the two data sets. The HRF of the two genuine data sets is evident in left and right panels of Figure 5 to be "monotonically growing." The left and right panels of Figure 6 prove that there are no extreme values. The fits of the QPGWL are contrasted with those of numerous popular Lomax extensions, including the odd log-logistic Lomax (OLLL), special generalized mixture Lomax (SGML), reduced odd log-logistic Lomax (ROLLL), reduced Burr-Hatke Lomax (RBHL), gamma Lomax (GL), transmuted Topp-Leone Lomax (TTLL), reduced transmuted Topp-Leone Lomax (RTTLL) and beta Lomax (BL). The following goodness-of-fit (GOF) statistics are used for comparing competitive models:

1.   The "Akaike information" (AICr).
2.   The "consistent-AIC" (CAICr).
3.   The "Bayesian-IC" (BICr).
4.   The "Hannan-Quinn-IC" (HQICr).

The MLEs and corresponding standard errors (SEs) for the two data sets are provided in Tables 1 and 3, respectively. Results of the four GOF statistic tests for the two data sets are presented in Tables 2 and 4, respectively. For the first data set, Figure 7 shows the fitted CDF, fitted density, Kaplan-Meier Survival (KMS) plot, Probability- Probability (P-P) plot, and estimated HRF (EHRF). For the second data set, Figure 8 displays the FCDF, fitted density, P-P plot, KMS plot, and EHRF.

Based on Tables 2 and 4, it is noted that the QPGWL model gives the lowest values for all GOF statistic tests with AICr=**263.303**, CAICr = **263.603**, BICr = **270.5954** and HQICr = **266.2345** for the first data, and AICr = **204.501**, CAICr = **204.908**, BICr = **210.931** and HQICr = **207.030** for the second data among all fitted competitive models. So, it could be selected as the best extension under these four GOF criteria.
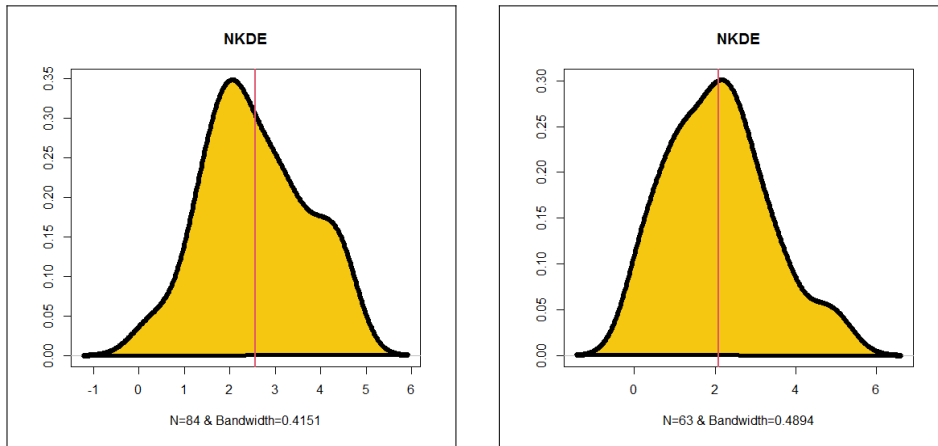
1ˢᵗ data   **2ⁿᵈ data**

Figure 3: NKDE plots**.**
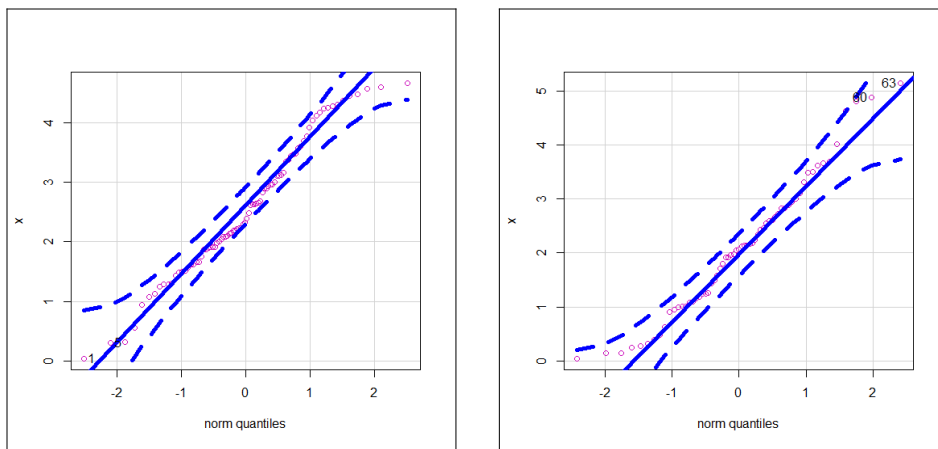
1ˢᵗ data   **2ⁿᵈ data**

Figure 4: Q-Q plots**.**
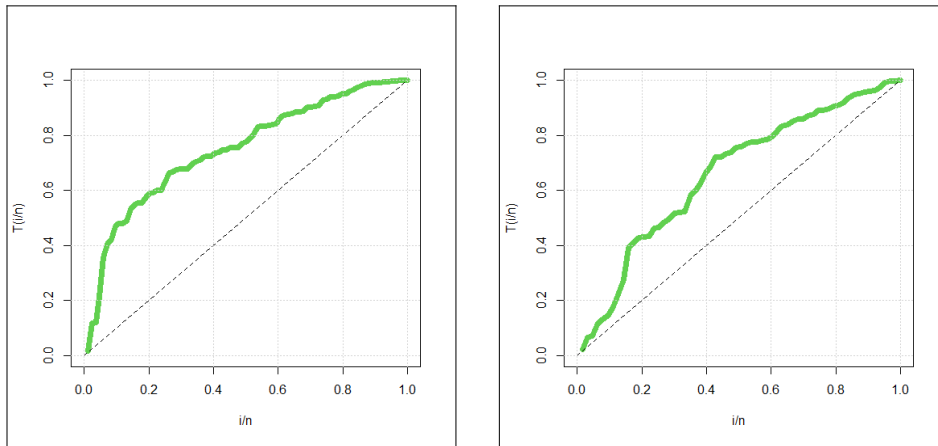
1st data   **2nd** data

Figure 5: TTT plots
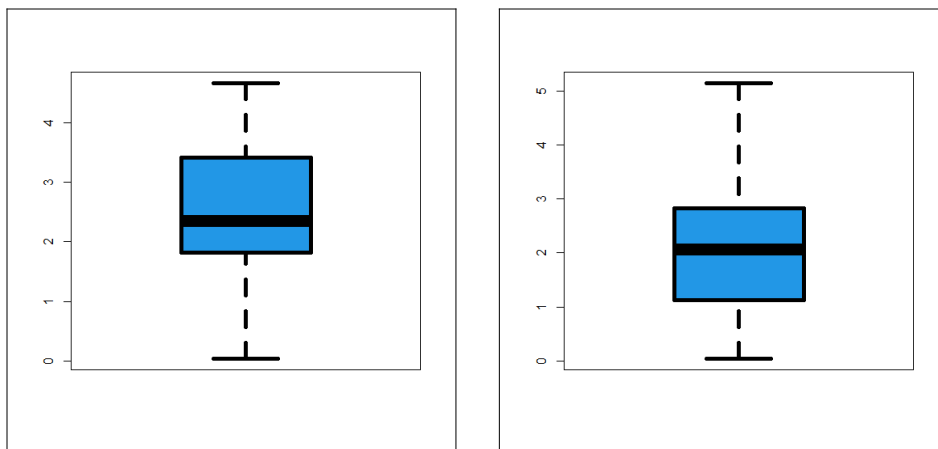
1st data   **2nd** data

Figure 6: Box plots

Table 1: MLEs and corresponding SEs for **1st** data.

Model	Estimates			
QPGWL(a, b, π)	**0.28667**	**8.86699**	**0.4202**	
	(0.0278)	**(0.0028)**	**(0.003)**	
KL(a, b, α, π)	2.6150	100.276	5.27710	78.6774
	(0.3822)	(120.49)	(9.8116)	(186.01)
TTLL(a, b, α, π)	-0.8075	2.47663	(15608)	(38628)
	(0.1396)	(0.5418)	(1602.4)	(123.94)
BL(a, b, α, π)	3.60360	33.6387	4.83070	118.837
	(0.6187)	(63.715)	(9.2382)	(428.93)
PRHRL(a, b, π)	3.73×10^6	4.71×10^{-1}	4.5×10^6	
	1.01×10^6	(0.00001)	37.1468	
SGML(a, b, π)	-1.04×10^{-1}	9.83×10^6	1.18×10^7	
	(0.1223)	(4843.3)	(501.04)	

RTTLL(a,b,π)	-0.84732	5.52057	1.15678
	(0.1001)	(1.1848)	(0.0959)
OLLL(a,b,π)	2.32636	7.17×10^5	2.3×10^6
	(2.14×10^{-1})	(1.19×10^4)	(2.6×10^1)
exp-L(a,b,π)	3.62610	20074.5	26257.7
	(0.6236)	(2041.8)	(99.74)
GL(a,b,π)	3.58760	52001.4	37029.7
	(0.5133)	(7955.0)	(81.16)
ROLLL(a,π)	3.89056	0.57316	
	(0.3652)	(0.0195)	
RBHL(a,π)	1080175	513672	
	(983309)	(23231)	
L(a,π)	51425.4	131790	
	(5933.5)	(296.12)	

Table 2: GOF statistic tests for first data.

Model	AICr	BICr	CAICr	HQICr
QPGWL	**263.303**	**270.5954**	**263.603**	**266.2345**
OLLL	274.847	282.139	275.147	277.779
TTLL	279.140	288.863	279.646	283.049
GL	282.808	290.136	283.105	285.756
BL	285.435	295.206	285.935	289.365
exp-L	288.799	296.127	289.096	291.747
ROLLL	289.690	294.552	289.839	291.645
SGML	292.175	299.467	292.475	295.106
RTTLL	313.962	321.254	314.262	316.893
PRHRL	331.754	339.046	332.054	334.686
L	333.977	338.862	334.123	335.942
RBHL	341.208	346.070	341.356	343.162

Table 3: MLEs and corresponding SEs for second data.

Model	Estimates			
QPGWL(a,b,π)	**0.1985**	**8.0878**	**0.4143**	
	(0.0231)	**(0.0223)**	**(0.0113)**	
BL(a,b,α,π)	1.9218	31.2594	4.9684	169.572
	(0.318)	(316.84)	(50.528)	(339.21)
KL(a,b,α,π)	1.6691	60.5673	2.56490	65.0640
	(0.257)	(86.013)	(4.7589)	(177.59)
TTLL(a,b,α,π)	(-0.607)	1.78578	2123.39	4822.79
	(0.2137)	(0.4152)	(163.92)	(200.01)
RTTLL(a,b,π)	-0.6715	2.74496	1.01238	
	(0.18746)	(0.6696)	(0.1141)	
PRHRL(a,b,π)	1.59×10^6	3.93×10^{-1}	1.30×10^6	
	2.01×10^3	0.0004×10^{-1}	0.95×10^6	
SGML(a,b,π)	-1.04×10^{-1}	6.45×10^6	6.33×10^6	
	(4.1×10^{-10})	(3.21×10^6)	(3.8573)	
GL(a,b,π)	1.9073	35842.433	39197.57	
	(0.3213)	(6945.074)	(151.653)	
OLLL(a,b,π)	1.66419	6.340×10^5	2.01×10^6	
	(1.8×10^{-1})	(1.68×10^4)	7.22×10^6	
exp-L(a,b,π)	1.9145	22971.15	32882.0	
	(0.348)	(3209.53)	(162.22)	

RBHL(a, π)	14055522	53203423
	(422.01)	(28.5232)
ROLLL(a, π)	2.372333	0.691092
	(0.2683)	(0.0449)
L(a, π)	99269.79	207019.36
	(11863.9)	(301.2371)

Table 4: GOF statistic tests for second data.

Model	AICr	BICr	CAICr	HQICr
QPGWL	**204.501**	**210.931**	**204.908**	**207.030**
KL	209.735	218.308	210.425	213.107
TTLL	212.900	221.472	213.589	216.271
GL	211.666	218.096	212.073	214.195
SGML	211.788	218.218	212.195	214.317
BL	213.922	222.495	214.612	217.294
exp-L	213.099	219.529	213.506	215.628
OLLL	215.808	222.238	216.215	218.337
PRHRL	224.597	231.027	225.004	227.126
L	222.598	226.884	222.798	224.283
ROLLL	225.457	229.744	225.657	227.143
RTTLL	230.371	236.800	230.778	232.900
RBHL	229.201	233.487	229.401	230.887
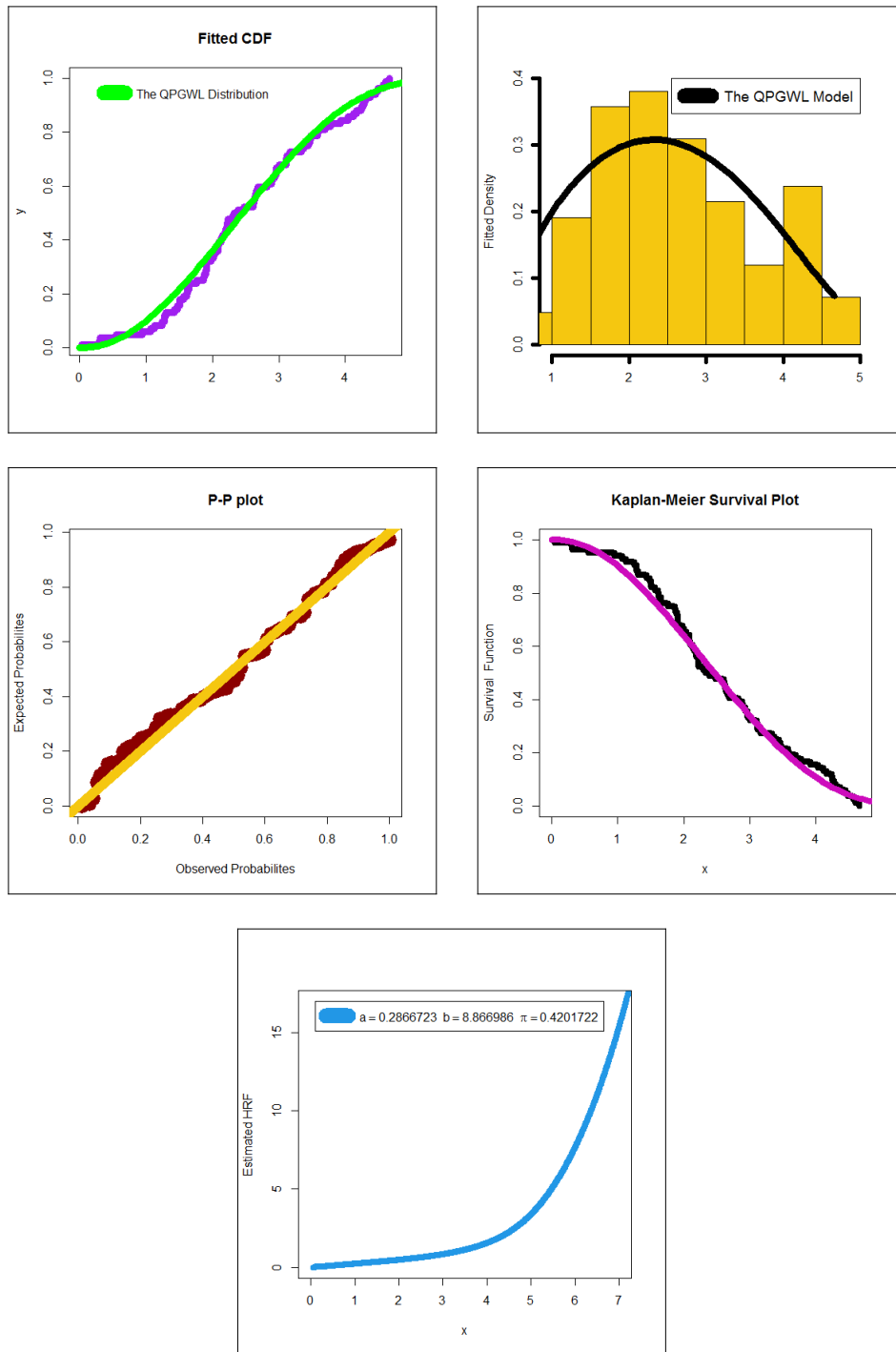
Figure 7: Fitted CDF and PDF, P-P, KMS plots and EHRF for the first data.
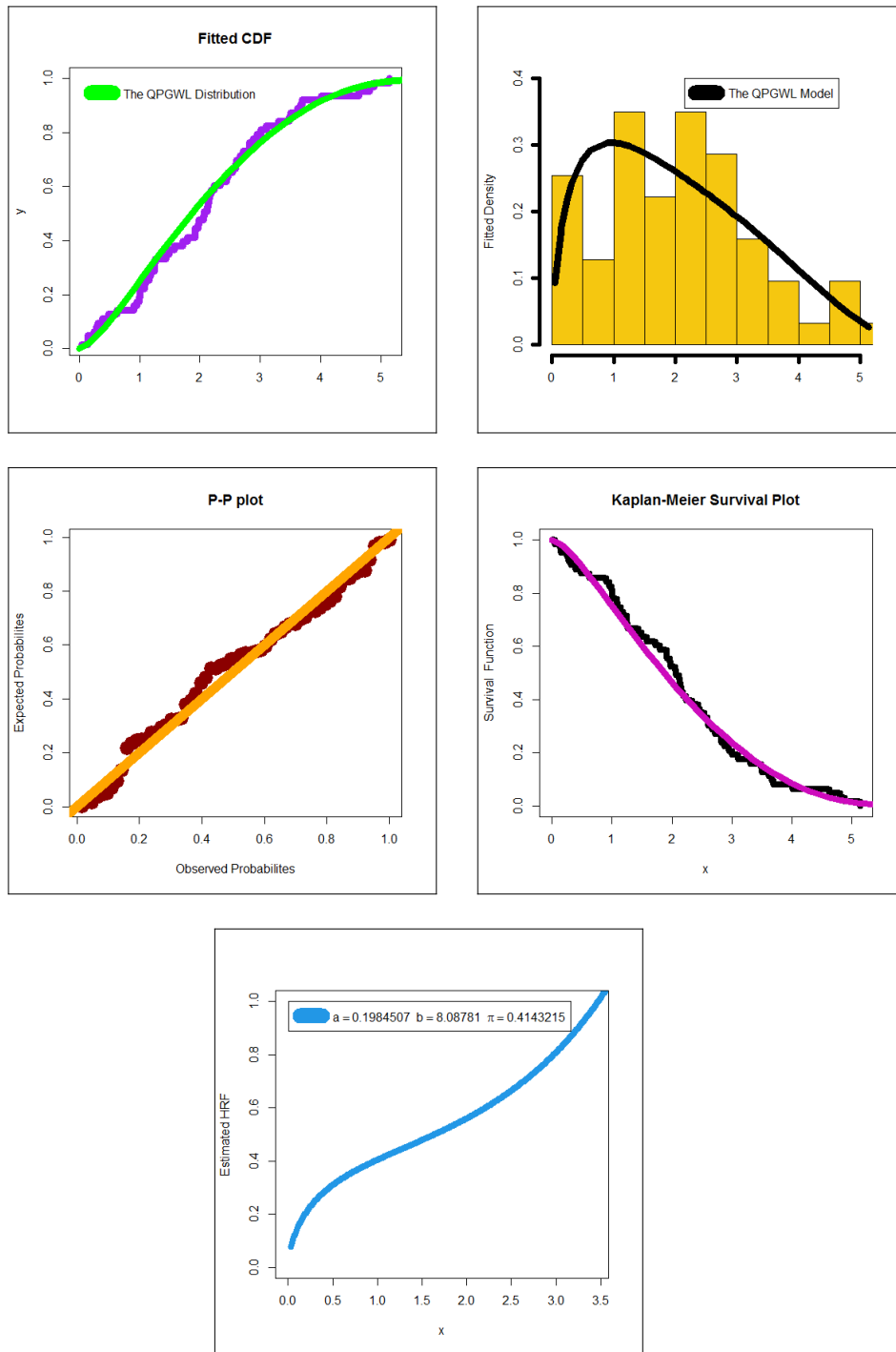
Figure 8: Fitted CDF and PDF, P-P, KMS plots and EHRF for the second data set.

7. Risk analysis under insurance claims data

The temporal growth of claims through time for each appropriate exposure (or origin) period is frequently shown in the historical insurance actual data in the form of a triangle presentation. The year the insurance policy was purchased or the time period during which the loss occurred may be regarded as the exposure period. It is obvious that the origin period need not be annual. For instance, it may be monthly or quarterly origin periods. The development time of an origin period is referred to as the claim age or claim lag. Data from separate insurance is frequently combined to represent uniform company lines, division levels, or risks.

We examine the insurance claims payment triangle from a U.K. Motor Non-Comprehensive account in this paper as a practical illustration. We choose to set the origin period from 2007 to 2013 because of convenience (see Charpentier (2014)). The insurance claims payment data frame displays the claims data in the manner in which a database would normally keep it. The origin year, which ranges from 2007 to 2013, the development year, and the incremental payments are all listed in the first column. It's important to note that this data on insurance claims was initially examined using a probability-based distribution.

Again, but for the claim's insurance data, we examine the statistics on insurance claims first. Real data analysis can be carried out visually, quantitatively, or by combining the two. The numerical method as well as several graphical tools, like as the skewness-kurtosis plot (or the Cullen and Frey plot), are taken into consideration when analyzing initial fits of theoretical distributions such the normal, uniform, exponential, logistic, beta, lognormal, and Weibull (see Figure 9). We have left-skewed data with a kurtosis of less than three, as shown in Figure 9.

In light of this, numerous additional graphical techniques are taken into consideration, including the NKDE approach for investigating the initial shape of the insurance claims density (see Figure 10, the top left plot), the Q-Q plot for investigating the "normality" of the current data (see Figure 10, the top right plot), the TTT plot for investigating the initial shape of the empirical HRF (see Figure 10, the bottom left plot), and the "box plot" for identifying the extreme claims (see Figure 10, the bottom right plot).

Figure 10 (top left plot) shows that the initial density is an asymmetric function with left tail. No extreme claims are spotted based on Figure 10 (bottom right plot). Further, Figure 10 (bottom left plot) indicates that the HRF for the models to explain the current data should be monotonically increasing. Figure 11 presents the scattergrams for the insurance claims data. Figure 12 (left plot) presents autocorrelation function (the ACF), and Figure 12 (right plot) presents the partial autocorrelation function (the partial ACF) for the insurance claims data. We present the ACF, which can be used to show how the correlation between any two signal values changes as their separation changes ACF. The theoretical ACF does not provide any insight into the frequency content of the process; rather, it is a time domain measure of the stochastic process memory. It provides some information about the distribution of hills and valleys across the surface with Lag $= k = 1$; see Figure 12 (the left plot). The theoretical partial ACF with Lag $= k = 1$ is also given; see Figure 12 (the right plot). Figure 12 (the right plot) reveals that the first lag value is statistically significant, whereas the other partial autocorrelations for all other lags are not statistically significant. Based on Figure 10 (the top left panel), the initial NKDE is an asymmetric density with left tail. On the other hand, the density of the novel model contains the left tail shape, this matching and this interview is important in statistical modeling. Hence, the QPGWL model is recommended for model the insurance claim's payments data.

We present an application for risk analysis under VaR, TVaR, TV, TMV and EL measures for the insurance claims data. The risk analysis is done for some confidence level as follows:

$$q = 60\%, 65\%, 70\%, 75\%, 80\%, 85\%, 90\%, 95\%, 99\% \text{ and } 99.9\%.$$

The five measures are estimated for the QPGWL and GWL models. The GWL model is the better model for this application. Table 5 reports the KRIs for the QPGWL and GWL models. The GWL distribution was chosen because it is the base line distribution on which the new distribution is based. For the QPGWL model, the quantity of the VaRq $(Z; a, b, \pi)$ ranges from $0.06108605|q = 60\%$ to $0.46051700|q = 99.9\%$, however, for the GWL model, the quantity VaRq $(Z; a, b, \pi)$ ranges from $0.03405504|q = 60\%$ to $0.10564970|q = 99.9\%$. The TVaRq $(Z; a, b, \pi)$ ranges from $0.1277527|q = 60\%$ to $0.5271837|q = 99.9\%$. However, for the GWL model, the quantity TVaRq $(Z; a, b, \pi)$ ranges from $0.1007217|q = 60\%$ to $0.1723164|q = 99.9\%$. The TVq $(Z; a, b, \pi)$ for the QPGWL model= TVq

$(Z; a, b, \pi)$ for the GWL model= $0.004444444 \, \forall \, q$. The TMVq $(Z; a, b, \pi, 0.99)$ for the QPGWL model ranges from $0.1321527|q = 60\%$ to $0.5315837|q = 99.9\%$. However, for the GWL model, the quantity TMVq $(Z; a, b, \pi, 0.99)$ ranges from $0.1051217|q = 60\%$ to $0.1767164|q = 99.9\%$. Further, $\forall q$, ELq $(Z; \eta, \psi)$ is evaluated and it is seen that ELq$(Z; a, b, \pi)$ for the QPGWL model $=$ ELq$(Z; a, b, \pi)$ for the GWL model $\forall \, q$. In addition, we can list the following results:

$$\text{VaRq}(Z; a, b, \pi) \text{ for QPGWL model} > \text{VaRq}(Z; a, b, \pi) \text{ for GWL model} \, \forall \, q,$$

$$\text{TVaRq}(Z; a, b, \pi) \text{ for QPGWL model} > \text{TVaRq}(Z; a, b, \pi) \text{ for GWL model} \, \forall \, q,$$

$$\text{TVq}(Z; a, b, \pi) \text{ for QPGWL model} = \text{TVq}(Z; a, b, \pi) \text{ for GWL model} \, \forall \, q,$$

$$\text{TMVq}(Z; a, b, \pi, 0.99) \text{ for QPGWL model} > \text{TMVq}(Z; a, b, \pi, 0.99) \text{ for GWL model} \, \forall \, q,$$

$$\text{VaRq}(Z; a, b, \pi) < \text{TVaRq}(Z; a, b, \pi) < \text{TMVq}(Z; a, b, \pi) \, \forall \, q.$$

VaRq for QPGWL $|q = 60\% <$ VaRq for QPGWL $|q = 65\% < \ldots <$ VaRq for QPGWL $|q = 99.9\%$,

VaRq for GWL $|q = 60\% <$ VaRq for GWL $|q = 65\% < \ldots <$ VaRq for GWL $|q = 99.9\%$,

TVaRq for QPGWL $|q = 60\% <$ TVaRq for QPGWL $|q = 65\% < \ldots <$ TVaRq for QPGWL $|q = 99.9\%$,

TVaRq for GWL $|q = 60\% <$ TVaRq for GWL $|q = 65\% < \ldots <$ TVaRq for GWL $|q = 99.9\%$,

TMVq for QPGWL $|q = 60\% <$ TMVq for QPGWL $|q = 65\% < \ldots <$ TVaRq for QPGWL $|q = 99.9\%$,

TMVq for GWL $|q = 60\% <$ TMVq for GWL $|q = 65\% < \ldots <$ TMVq for GWL $|q = 99.9\%$,
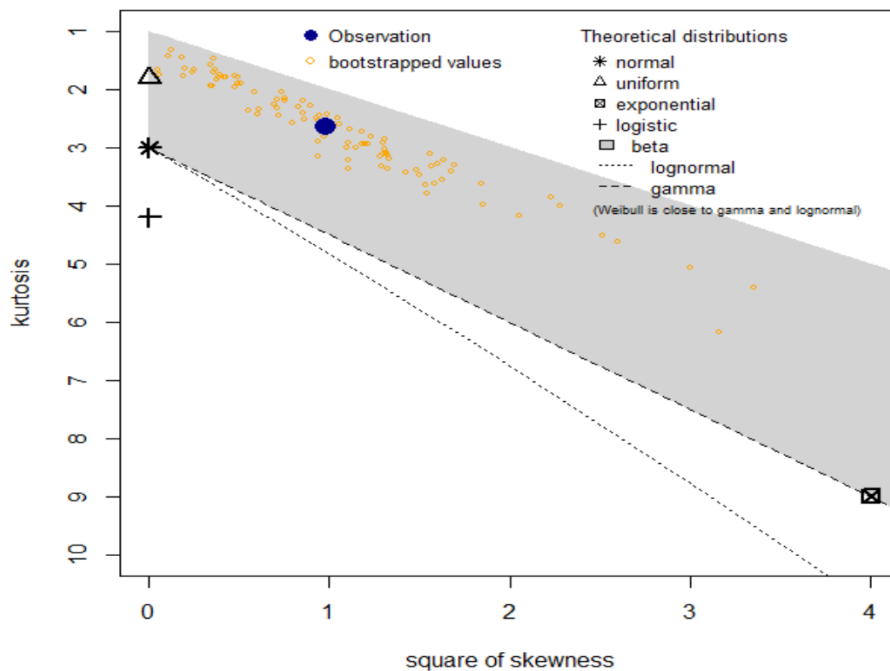
Figure 9: Cullen and Frey plot for the claims data.

Figure 13 gives VaRq, TVaRq, TMVq and its corresponding Q-Q plots for QPGWL and GWL models respectively. Figure 13 (first column) represents the VaRq, TVaRq, TMVq for the two competitive models. Figure 13 (second column) shows the Q-Q plots for the VaRq, TVaRq, TMVq for the QPGWL model. Figure 13 (second column) gives the Q-Q plots for the VaRq, TVaRq, TMVq for the GWL model. Each plot of Figure 13 (first column) provides a graphical comparison between QPGWL and GWL models. Based on Figure 11m, the QPGWL model has a heavier tail than the GWL distribution for all KRIs.
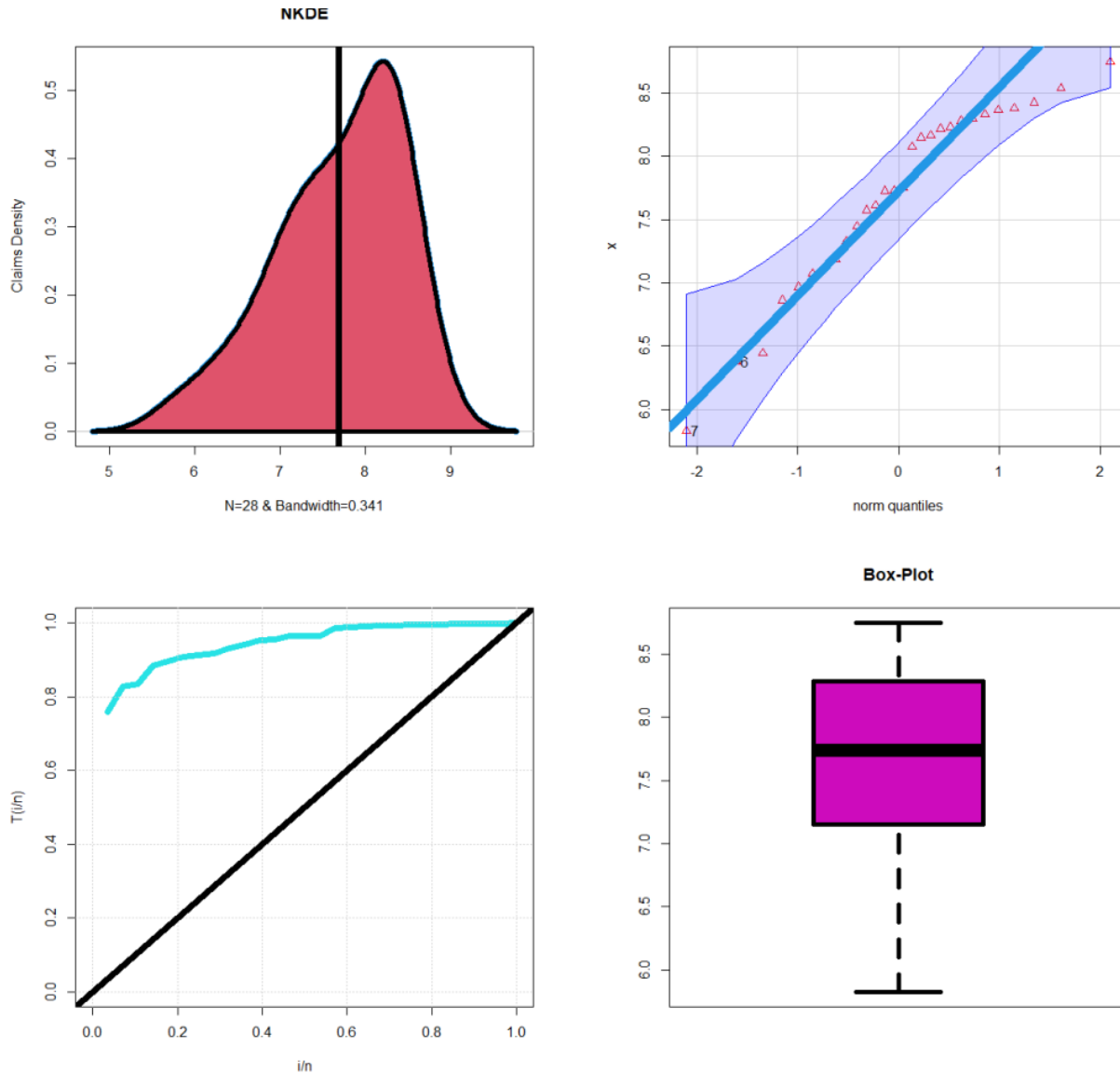
Figure 10: NKDE, Q-Q, TTT, box plots for the claims data.
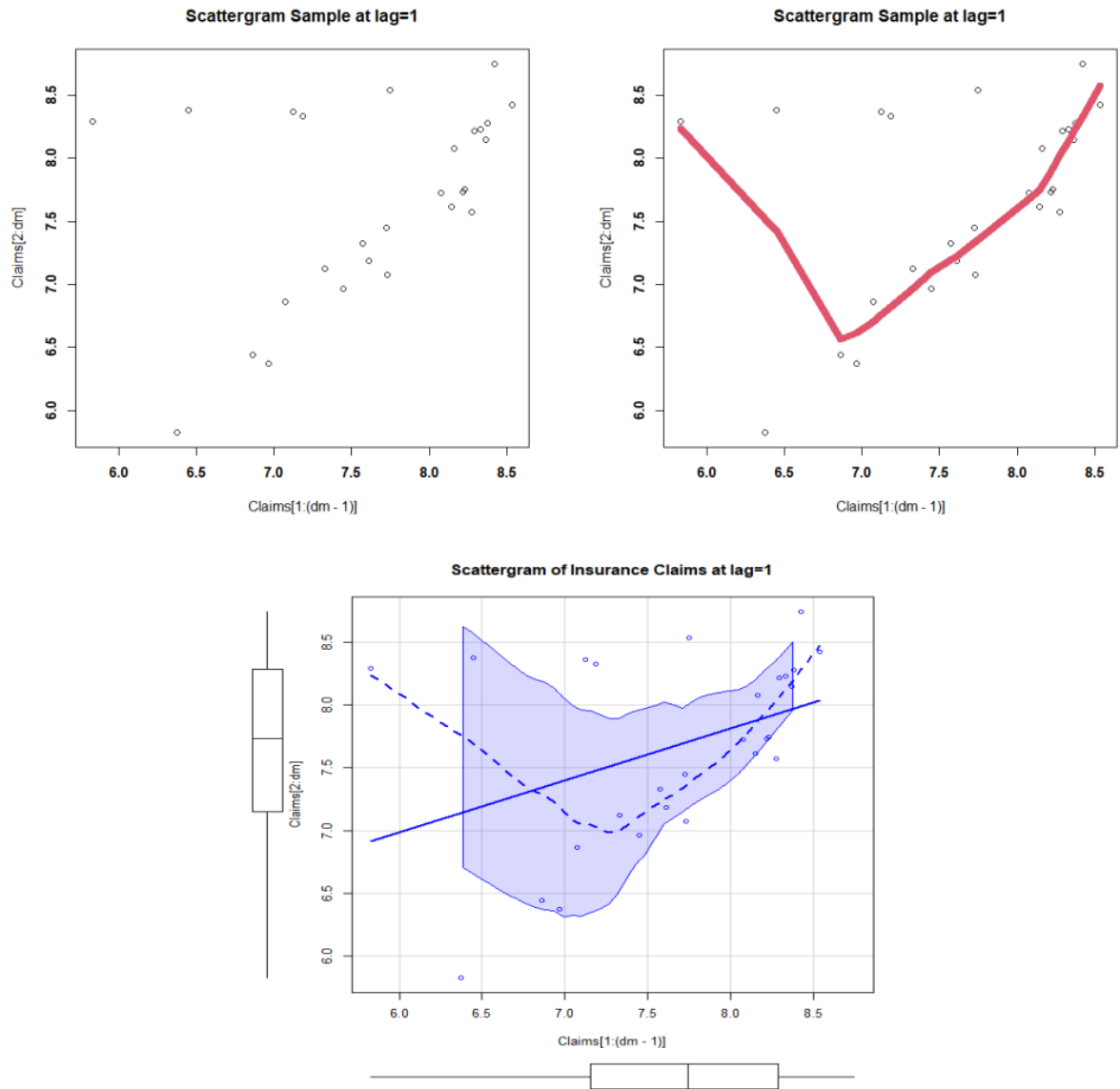
Figure 11: The scattergrams for the insurance claims data.
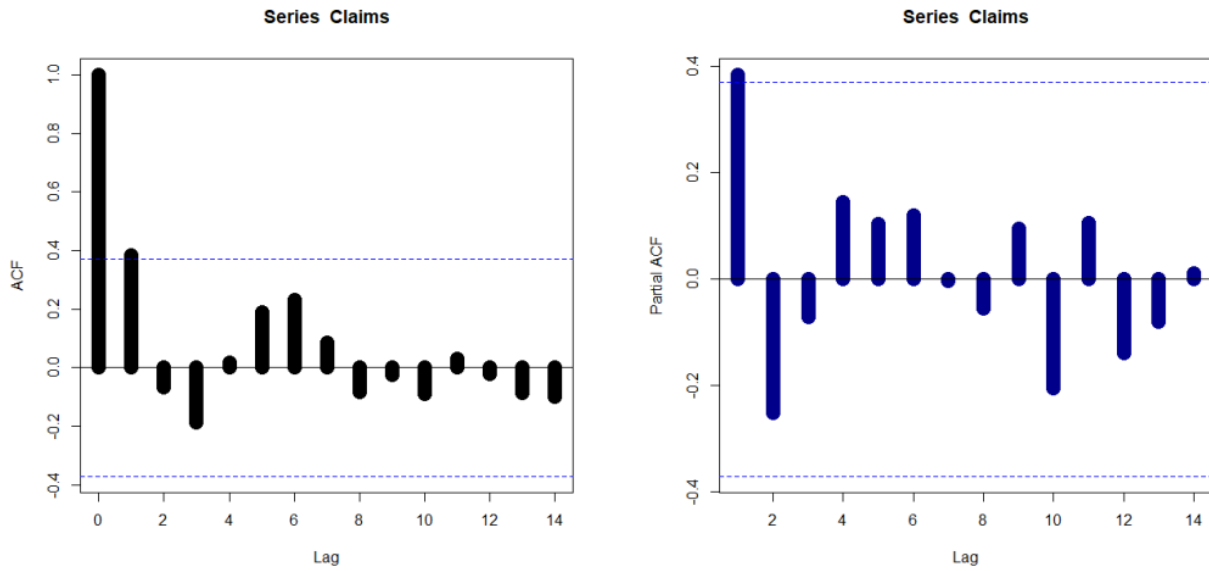
Figure 12: The ACF, and the partial ACF for the insurance claims data

Table 5: The KRIs for the QPGWL and GWL models.

q	VaRq$(Z; a, b, \pi)$	TVaRq$(Z; a, b, \pi)$	TVq$(Z; a, b, \pi)$	TMVq$(Z; a, b, \pi, 0.99)$	ELq$(Z; a, b, \pi)$
			QPGWL model		
60%	0.06108605	0.1277527	0.004444444	0.1321527	0.06666667
65%	0.06811008	0.1347767	0.004444444	0.1391767	0.06666667
70%	0.07807887	0.1447455	0.004444444	0.1491455	0.06666667
75%	0.08980491	0.1564716	0.004444444	0.1608716	0.06666667
80%	0.10729590	0.1739625	0.004444444	0.1783625	0.06666667
85%	0.12647470	0.1931413	0.004444444	0.1975413	0.06666667
90%	0.15350570	0.2201723	0.004444444	0.2245723	0.06666667
95%	0.19971550	0.2663822	0.004444444	0.2707822	0.06666667
99%	0.30701130	0.3736780	0.004444444	0.3780780	0.06666667
99.9%	0.46051700	0.5271837	0.004444444	0.5315837	0.06666667
			GWL model		
60%	0.03405504	0.1007217	0.004444444	0.1051217	0.06666667
65%	0.03747459	0.1041413	0.004444444	0.1085413	0.06666667
70%	0.04232522	0.1089919	0.004444444	0.1133919	0.06666667
75%	0.05033484	0.1170015	0.004444444	0.1214015	0.06666667
80%	0.05783337	0.1245000	0.004444444	0.1289000	0.06666667
85%	0.06363413	0.1303008	0.004444444	0.1347008	0.06666667
90%	0.06904250	0.1357092	0.004444444	0.1401092	0.06666667
95%	0.07916290	0.1458296	0.004444444	0.1502296	0.06666667
99%	0.08606561	0.1527323	0.004444444	0.1571323	0.06666667
99.9%	0.10564970	0.1723164	0.004444444	0.1767164	0.06666667
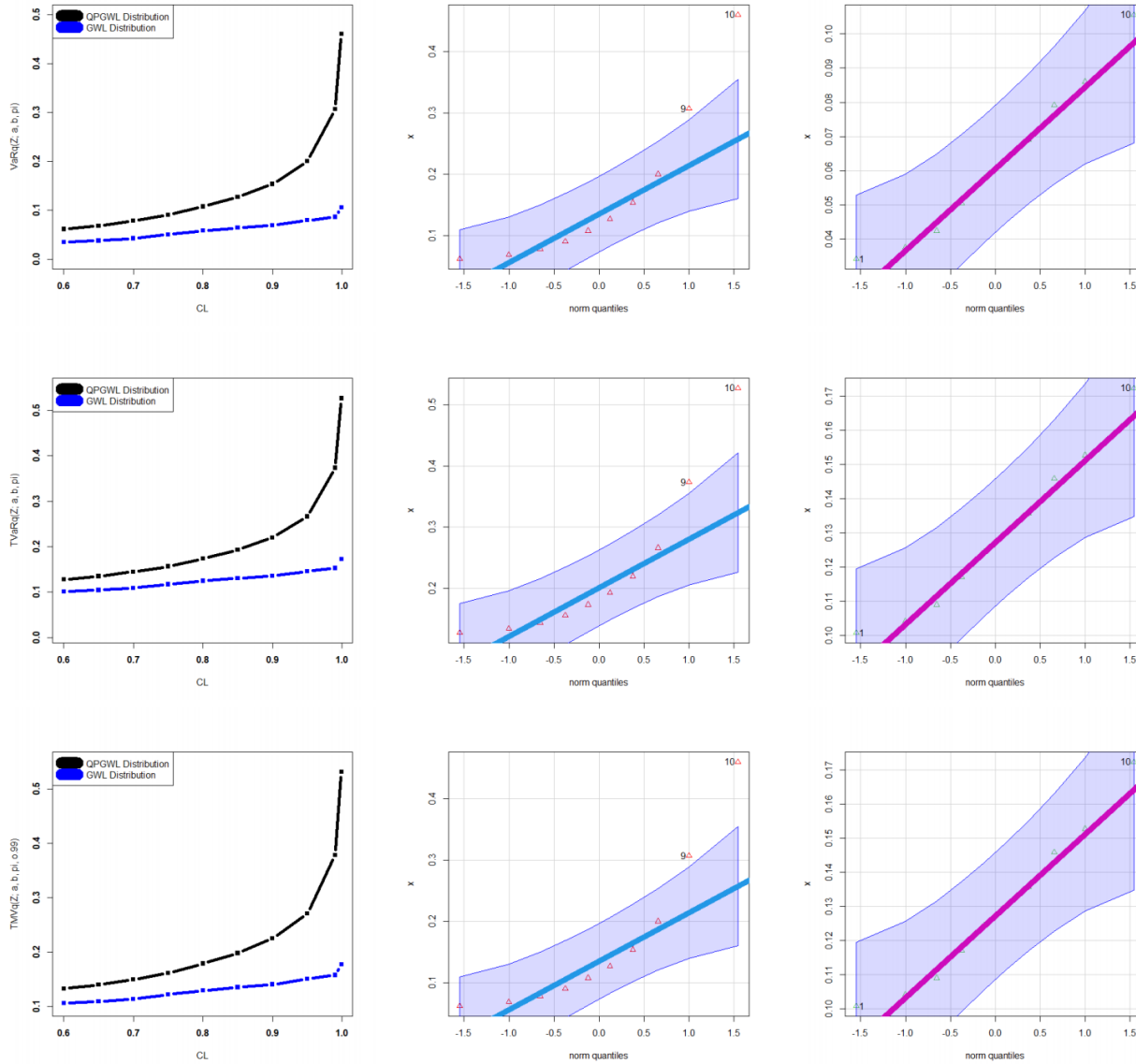
Figure 13: VaRq, TVaRq, TMVq and its corresponding Q-Q plots
for the QPGWL and GWL models, respectively.

8. Conclusions

The quasi-Poisson generalized Weibull Lomax distribution, a new three-parameter compound Lomax extension, is derived and examined in this study. Based on the generalized Weibull Lomax model and the compounding Poisson family, the quasi-Poisson generalized Weibull Lomax model is developed. The new density can be "monotonically declining," "symmetric," "bimodal-asymmetric," "asymmetric with right tail," "asymmetric with wide peak," or "asymmetric with left tail." The new hazard rate can take the following shapes: "J-shape," "bathtub (U-shape)," "upside down-increasing," "decreasing-constant," and "upside down-increasing." Relevant mathematical properties are determined, including mean waiting time, mean deviation, raw and incomplete moments, residual life moments, and moments of the reversed residual life. We used some common copulas, including the Farlie-Gumbel-Morgenstern copula, the Clayton copula, the modified Farlie-Gumbel-Morgenstern copula, and the Ali-Mikhail-Haq copula, to present some new bivariate quasi-Poisson generalized Weibull Lomax distributions for the bivariate mathematical modelling. Additionally, an application of the quasi-Poisson generalized Weibull Lomax distribution is reported by the analysis of two real data sets. Based on two real data sets, the Poisson exponentiated exponential Lomax model

gives the lowest statistic test with AICr=263.303, CAICr = 263.603, BICr = 270.5954 and HQICr = 266.2345 for the first data, and AICr = 204.501, CAICr = 204.908, BICr = 210.931 and HQICr = 207.030 for the second data among all fitted competitive models. So, it could be selected as the best extension under these four GOF criteria.

To represent count real-life data, it is suggested that a novel discrete quasi-Poisson generalized Weibull Lomax model be presented; for more details, see Aboraya et al. (2020), Chesneau et al. (2022), Yousof et al. (2021), and Ibrahim et al. (2022b). Additionally, using the Bagdonaviius-Nikulin and Nikulin-Rao-Robson tests, see, for example, Ibrahim et al. (2019), Goual et al. (2019, 2020), Yadav et al. (2020 and 2022), Ibrahim et al. (2022a), Goual and Yousof (2020), Aidi et al. (2021) and Yousof et al. (2022)). Following Altun et al. (2018a,b) and Yousof et al. (2019) and under the quasi-Poisson generalized Weibull Lomax distribution, some new developments of certain new regression models for modelling censored data sets. The generalized stress-strength parameter under the quasi-Poisson generalized Weibull Lomax model could be inferred using Bayesian and classical methods due to Saber and Yousof (2022) as well as reliability estimation for the remained stress-strength model under the quasi-Poisson generalized Weibull Lomax distribution due to Saber et al. (2022). A single acceptance sampling strategy with its associated application in quality and risk decisions might be given in the manner of Ahmed and Yousof (2022) and Ahmed et al. (2022). Finally, one might follow Mohamed et al. (2022a,b,c) to find applications for more insurance studies under some time series models such as Autoregressive (AR) models, moving average (MA) models, autoregressive moving average (ARMA) modes and autoregressive integrated moving average (ARIMA) models.

References

1. Aboraya, M., Ali, M. M., Yousof, H. M. and Ibrahim, M. (2022). A novel Lomax extension with statistical properties, copulas, different estimation methods and applications. Bulletin of the Malaysian Mathematical Sciences Society, (2022) https://doi.org/10.1007/s40840-022-01250-y
2. Aboraya, M., M. Yousof, H. M., Hamedani, G. G. and Ibrahim, M. (2020). A new family of discrete distributions with mathematical properties, characterizations, Bayesian and non-Bayesian estimation methods. Mathematics, 8, 1648.
3. Acerbi, C. and Tasche, D. (2002), On the coherence of expected shortfall, Journal of Banking and Finance, 26, 1487-1503.
4. Ahmed, B., Ali, M. M. and Yousof, H. M. (2022). A novel G family for single acceptance sampling pan with application in quality and risk decisions, Annals of Data Science, forthcoming.
5. Ahmed, B. and Yousof, H. M. (2022). A new group acceptance sampling plans based on percentiles for the Weibull Fréchet model. Statistics, Optimization & Information Computing, forthcoming.
6. Aidi, K., Butt, N. S., Ali, M. M., Ibrahim, M., Yousof, H. M. and Shehata, W. A. M. (2021). A modified Chi-square type test statistic for the double Burr X model with applications to right censored medical and reliability data. Pakistan Journal of Statistics and Operation Research, 17, 615-623.
7. Al-babtan, A. A., Elbatal, I. and Yousof, H. M. (2020a). A new flexible three-parameter model: properties, Clayton copula, and modeling real data. Symmetry, 12, 440.
8. Al-Babtain, A. A., Elbatal, I. and Yousof, H. M. (2020b). A new three parameter Fréchet model with mathematical properties and applications. Journal of Taibah University for Science, 14, 265-278.
9. Ali, M. M., Ibrahim, M. and Yousof, H. M. (2021a). Expanding the Burr X model: properties, copula, real data modeling and different methods of estimation. Optimal Decision Making in Operations Research & Statistics: Methodologies and Applications, CRC Press, 21-42.
10. Ali, M. M., Mikhail, N. N. and Haq, M. S. (1978). A class of bivariate distributions including the bivariate logistic. Journal of multivariate analysis, 8, 405-412.
11. Ali, M. M., Yousof, H. M. and Ibrahim, M. (2021b). A new version of the generalized Rayleigh distribution with copula, properties, applications and different methods of estimation. Optimal Decision Making in Operations Research & Statistics: Methodologies and Applications, CRC Press, 1-20.
12. Alizadeh, M., Jamal, F., Yousof, H. M., Khanahmadi, M. and Hamedani, G. G. (2020a). Flexible Weibull generated family of distributions: characterizations, mathematical properties and applications. University Politehnica of Bucharest Scientific Bulletin-Series A-Applied Mathematics and Physics, 82, 145-150.
13. Alizadeh, M., Rasekhi, M., Yousof, H. M., Ramires, T. G. and Hamedani G. G. (2018). Extended exponentiated Nadarajah-Haghighi model: mathematical properties, characterizations and applications. Studia Scientiarum Mathematicarum Hungarica, 55, 498-522.
14. Alizadeh, M., Yousof, H. M., Jahanshahi, S. M. A., Najibi, S. M. and Hamedani, G. G. (2020b). The transmuted

odd log-logistic-G family of distributions. Journal of Statistics and Management Systems, 23, 1-27.

15. Altun, E., Yousof, H. M. and Hamedani, G. G. (2018a). A new log-location regression model with influence diagnostics and residual analysis. Facta Universitatis, Series: Mathematics and Informatics, 33, 417-449.

16. Almazah, M.M.A., Almuqrin, M.A., Eliwa, M.S., El-Morshedy, M., Yousof, H.M. (2021). Modeling Extreme Values Utilizing an Asymmetric Probability Function. Symmetry, 13, 1730.

17. Altun, E., Yousof, H. M., Chakraborty, S. and Handique, L. (2018b). Zografos-Balakrishnan Burr XII distribution: regression modeling and applications. International Journal of Mathematics and Statistics, 19, 46-70.

18. Aryal, G. R. and Yousof, H. M. (2017). The exponentiated generalized-G Poisson family of distributions. Economic Quality Control, 32, 1-17.

19. Aryal, G. R., Ortega, E. M., Hamedani, G. G. and Yousof, H. M. (2017). The Topp-Leone generated Weibull distribution: regression model, characterizations and applications. International Journal of Statistics and Probability, 6, 126-141.

20. Asgharzadeh, A. and Valiollahi, R. (2011). Estimation of the scale parameter of the Lomax distribution under progressive censoring, International Journal for Business and Economics 6, 37-48.

21. Burr, I. W. (1942). Cumulative frequency functions. Annals of Mathematical Statistics, 13, 215-232.

22. Burr, I. W. (1968). On a general system of distributions, III. The simple range. Journal of the American Statistical Association, 63, 636-643.

23. Burr, I. W. (1973). Parameters for a general system of distributions to match a grid of α_3 and α_4. Communications in Statistics, 2, 1-21.

24. Burr, I. W. and Cislak, P. J. (1968). On a general system of distributions: I. Its curve-shaped characteristics; II. The sample median. Journalof the American Statistical Association, 63, 627-635.

25. Chesneau, C. and Yousof, H. M. (2021), On a special generalized mixture class of probabilistic models. Journal of Nonlinear Modeling and Analysis, 3, 71-92.

26. Chesneau, C., Yousof, H. M., Hamedani, G. and Ibrahim, M. (2022). A New One-parameter Discrete Distribution: The Discrete Inverse Burr Distribution: Characterizations, Properties, Applications, Bayesian and Non-Bayesian Estimations. Statistics, Optimization & Information Computing, 10, 352-371.

27. Corbellini, A., Crosato, L., Ganugi, P. and Mazzoli, M. (2010). Fitting Pareto II distributions on firm size: Statistical methodology and economic puzzles. In Advances in Data Analysis (pp. 321-328). Birkhäuser Boston.

28. Cordeiro, G. M., Ortega, E. M. and Popovic, B. V. (2015). The gamma-Lomax distribution. Journal of Statistical computation and Simulation, 85, 305-319.

29. Cramer, E. and Schemiedt, A.B. (2011). Progressively type-II censored competing risks data from Lomax distribution, Computational Statistics and Data Analysis 55, 1285–1303.

30. Elgohari, H. and Yousof, H. M. (2020a). A generalization of Lomax distribution with properties, copula and real data applications. Pakistan Journal of Statistics and Operation Research, 16, 697-711.

31. Elgohari, H. and Yousof, H. M. (2021). A new extreme value model with different copula, statistical properties and applications. Pakistan Journal of Statistics and Operation Research, 17, 1015-1035.

32. Elgohari, H. and Yousof, H. M. (2020b). New extension of Weibull distribution: copula, mathematical properties and data modeling. Statistics, Optimization & Information Computing, 8, 972-993.

33. Elgohari, H., Ibrahim, M. and Yousof, H. M. (2021). A new probability distribution for modeling failure and service times: properties, copulas and various estimation methods. Statistics, Optimization & Information Computing, 8(3), 555-586.

34. Figueiredo, F., Gomes, M. I. and Henriques-Rodrigues, L. (2017). Value-at-risk estimation and the PORT mean-of-order-p methodology. Revstat, 15, 187-204.

35. Furman, E., Landsman, Z. (2006). Tail variance premium with applications for elliptical portfolio of risks. ASTIN Bulletin, 36, 433-462.

36. Farlie, D. J. G. (1960). The performance of some correlation coefficients for a general bivariate distribution. Biometrika, 47, 307-323.

37. Charpentier, A. (2014). Computational actuarial science with R. CRC press.

38. Goual, H., Yousof, H. M. and Ali, M. M. (2019). Validation of the odd Lindley exponentiated exponential by a modified goodness of fit test with applications to censored and complete data. Pakistan Journal of Statistics and Operation Research, 15, 745-771.

39. Goual, H. and Yousof, H. M. (2020). Validation of Burr XII inverse Rayleigh model via a modified chi-squared goodness-of-fit test. Journal of Applied Statistics, 47, 393-423.

40. Goual, H., Yousof, H. M. and Ali, M. M. (2020). Lomax inverse Weibull model: properties, applications, and a modified Chi-squared goodness-of-fit test for validation. Journal of Nonlinear Sciences & Applications, 13(6),

330-353.

41. Gupta, R. C., Gupta, P. L. and Gupta, R. D. (1998). Modeling failure time data by Lehman alternatives. Communications in Statistics-Theory and methods, 27, 887-904.

42. Gumbel, E. J. (1961). Bivariate logistic distributions. Journal of the American Statistical Association, 56, 335-349.

43. Gumbel, E. J. (1960) Bivariate exponential distributions. Journ. Amer. Statist. Assoc., 55, 698-707.

44. Hamedani, G. G., Altun, E, Korkmaz, M. C., Yousof, H. M. and Butt, N. S. (2018). A new extended G family of continuous distributions with mathematical properties, characterizations and regression modeling. Pakistan Journal of Statistics and Operation Research, 14, 737-758.

45. Hamedani, G. G. Rasekhi, M., Najib, S. M., Yousof, H. M. and Alizadeh, M., (2019). Type II general exponential class of distributions. Pakistan Journal of Statistics and Operation Research, 15, 503-523.

46. Hamedani, G. G. Yousof, H. M., Rasekhi, M., Alizadeh, M., Najibi, S. M. (2017). Type I general exponential class of distributions. Pakistan Journal of Statistics and Operation Research, 14, 39-55.

47. Harris, C.M. (1968). The Pareto distribution as a queue service discipline, Operations Research 16, 307-313.

48. Hogg, R.V. and Klugman, S.A., 1984, Loss Distributions (New York: John Wiley & Sons, Inc.).

49. Ibragimov, R. amd Prokhorov, A. (2017). Heavy Tails and Copulas: Topics in Dependence Modelling in Economics and Finance; World Scientific: Singapore.

50. Ibrahim, M., Aidi, K., Ali, M. M. and Yousof, H. M. (2022a). A novel test statistic for right censored validity under a new Chen extension with applications in reliability and medicine. Annals of Data Science, forthcoming.

51. Ibrahim, M., Ali, M. M. and Yousof, H. M. (2022b). The discrete analogue of the Weibull G family: properties, different applications, Bayesian and non-Bayesian estimation methods. Annals of Data Science, forthcoming.

52. Ibrahim, M., Yadav, A. S., Yousof, H. M., Goual, H. and Hamedani, G. G. (2019). A new extension of Lindley distribution: modified validation test, characterizations and different methods of estimation. Communications for Statistical Applications and Methods, 26, 473-495.

53. Johnson, N. L. and Kotz, S. (1975) On some generalized Farlie-Gumbel-Morgenstern distributions. Commun. Stat. Theory, 4, 415-427.

54. Johnson, N. L. and Kotz, S. (1977) On some generalized Farlie-Gumbel-Morgenstern distributions- II: Regression, correlation and further generalizations. Commun. Stat.Theory, 6, 485-496.

55. Karamikabir, H., Afshari, M., Yousof, H. M., Alizadeh, M. and Hamedani, G. (2020). The Weibull Topp-Leone generated family of distributions: statistical properties and applications. Journal of The Iranian Statistical Society, 19, 121-161.

56. Korkmaz, M. Ç., Altun, E., Yousof, H. M. and Hamedani, G. G. (2020). The Hjorth's IDB generator of distributions: properties, characterizations, regression modeling and applications. Journal of Statistical Theory and Applications, 19, 59-74.

57. Korkmaz, M. C. Yousof, H. M. and Hamedani G. G. (2018a). The exponential Lindley odd log-logistic G family: properties, characterizations and applications. Journal of Statistical Theory and Applications, 17, 554 - 571.

58. Korkmaz, M. C., Yousof, H. M., Hamedani G. G. and Ali, M. M. (2018b). The Marshall–Olkin generalized G Poisson family of distributions, Pakistan Journal of Statistics, 34, 251-267.

59. Landsman, Z. (2010). On the tail mean--variance optimal portfolio selection. Insur. Math. Econ., 46, 547-553.

60. Lane, M.N. (2000). Pricing risk transfer transactions 1. ASTIN Bull. J. IAA, 30, 259-293.

61. Lemonte, A. J. and Cordeiro, G. M. (2013). An extended Lomax distribution. Statistics, 47, 800-816.

62. Lomax, K.S. (1954). Business failures: Another example of the analysis of failure data, Journal of the American Statistical Association 49, 847-852.

63. Mansour, M. M., Ibrahim, M., Aidi, K., Shafique Butt, N., Ali, M. M., Yousof, H. M. and Hamed, M. S. (2020a). A new log-logistic lifetime model with mathematical properties, copula, modified goodness-of-fit test for validation and real data modeling. Mathematics, 8, 1508.

64. Mansour, M. M., Butt, N. S., Ansari, S. I., Yousof, H. M., Ali, M. M. and Ibrahim, M. (2020b). A new exponentiated Weibull distribution's extension: copula, mathematical properties and applications. Contributions to Mathematics, 1, 57–66.

65. Mansour, M., Korkmaz, M. C., Ali, M. M., Yousof, H. M., Ansari, S. I. and Ibrahim, M. (2020c). A generalization of the exponentiated Weibull model with properties, Copula and application. Eurasian Bulletin of Mathematics, 3, 84-102.

66. Mansour, M., Rasekhi, M., Ibrahim, M., Aidi, K., Yousof, H. M. and Elrazik, E. A. (2020d). A new parametric life distribution with modified Bagdonavičius–Nikulin goodness-of-fit test for censored validation, properties, applications, and different estimation methods. Entropy, 22, 592.

67. Mansour, M., Yousof, H. M., Shehata, W. A. and Ibrahim, M. (2020e). A new two parameter Burr XII

distribution: properties, copula, different estimation methods and modeling acute bone cancer data. Journal of Nonlinear Science and Applications, 13, 223-238.

68. Mansour, M. M., Butt, N. S., Yousof, H. M., Ansari, S. I. and Ibrahim, M. (2020f). A generalization of reciprocal exponential model: clayton copula, statistical properties and modeling skewed and symmetric real data sets. Pakistan Journal of Statistics and Operation Research, 16, 373-386.

69. Merovci, F., Yousof, H. M. and Hamedani, G. G. (2020). The Poisson Topp Leone generator of distributions for lifetime data: theory, characterizations and applications. Pakistan Journal of Statistics and Operation Research, 16, 343-355.

70. Merovci, F., Alizadeh, M., Yousof, H. M. and Hamedani G. G. (2017). The exponentiated transmuted-G family of distributions: theory and applications, Communications in Statistics-Theory and Methods, 46, 10800-10822.

71. Mohamed, H. S., Cordeiro, G. M., and Yousof, H. M. (2022a). The synthetic autoregressive model for the insurance claims payment data: modeling and future prediction. Optimization & Information Computing, forthcoming.

72. Mohamed, H. S., Cordeiro, G. M., Minkah, R., Yousof, H. M. and Ibrahim, M. (2022b). A size-of-loss model for the negatively skewed insurance claims data: applications, risk analysis using different methods and statistical forecasting. Journal of Applied Statistics, forthcoming.

73. Mohamed, H. S., Ali, M. M. and Yousof, H. M. (2022c). The Lindley Gompertz Model for Estimating the Survival Rates: Properties and Applications in Insurance, Annals of Data Science, forthcoming.

74. Morgenstern, D. (1956). Einfache beispiele zweidimensionaler verteilungen. Mitteilungsblatt fur Mathematische Statistik, 8, 234-235.

75. Murthy, D.N.P. Xie, M. and Jiang, R. (2004). Weibull Models, Wiley.

76. Nascimento, A. D. C., Silva, K. F., Cordeiro, G. M., Alizadeh, M. and Yousof, H. M. (2019). The odd Nadarajah-Haghighi family of distributions: properties and applications. Studia Scientiarum Mathematicarum Hungarica, 56, 1-26.

77. Pougaza, D. B. and Djafari, M. A. (2011). Maximum entropies copulas. Proceedings of the 30th international workshop on Bayesian inference and maximum Entropy methods in Science and Engineering, 329-336.

78. Resnick, S.I. (1997), Discussion of the Danish data on large fire insurance losses. ASTIN Bulletin, 27, 139-151.

79. Rodriguez, R.N. (1977). A guide to the Burr type XII distributions. Biometrika, 64, 129-134.

80. Rodriguez-Lallena, J. A. and Ubeda-Flores, M. (2004). A new class of bivariate copulas. Statistics and Probability Letters, 66, 315-25.

81. Saber, M. M. and Yousof, H. M. (2022). Bayesian and classical tnference for generalized stress-strength parameter under generalized logistic distribution, Statistics, Optimization & Information Computing, forthcoming.

82. Saber, M. M. Marwa M. Mohie El-Din and Yousof, H. M. (2022). Reliability estimation for the remained stress-strength model under the generalized exponential lifetime distribution, Journal of Probability and Statistics, 2021, 1-10.

83. Shehata, W. A. M. and Yousof, H. M. (2021). The four-parameter exponentiated Weibull model with copula, properties and real data modeling. Pakistan Journal of Statistics and Operation Research, 17, 649-667.

84. Shehata, W. A. M. and Yousof, H. M. (2022). A novel two-parameter Nadarajah-Haghighi extension: properties, copulas, modeling real data and different estimation methods. Statistics, Optimization & Information Computing, 10, 725-749.

85. Shehata, W. A. M., Butt, N. S., Yousof, H. and Aboraya, M. (2022). A new lifetime parametric model for the survival and relief times with copulas and properties. Pakistan Journal of Statistics and Operation Research, 18, 249-272.

86. Shehata, W. A. M., Yousof, H. M. and Aboraya, M. (2021). A novel generator of continuous probability distributions for the asymmetric left-skewed bimodal real-life data with properties and copulas. Pakistan Journal of Statistics and Operation Research, 17, 943-961.

87. Stein, J. D., Lum, F., Lee, P. P., Rich III, W. L. and Coleman, A. L. (2014). Use of health care claims data to study patients with ophthalmologic conditions. Ophthalmology, 121, 1134-1141.

88. Tadikamalla, P. R. (1980). A look at the Burr and related distributions, International Statistical Review, 48, 337-344.

89. Tasche, D. (2002), Expected Shortfall and Beyond, Journal of Banking and Finance, 26, 1519-1533.

90. Wirch J. (1999), Raising Value at Risk,North American Actuarial Journal, 3, 106-115.

91. Yadav, A. S., Goual, H., Alotaibi, R. M., Ali, M. M. and Yousof, H. M. (2020). Validation of the Topp-Leone-Lomax model via a modified Nikulin-Rao-Robson goodness-of-fit test with different methods of estimation. Symmetry, 12, 57.

92. Yadav, A. S., Shukla, S., Goual, H., Saha, M. and Yousof, H. M. (2022). Validation of xgamma exponential model via Nikulin-Rao-Robson goodness-of- fit test under complete and censored sample with different methods of estimation. Statistics, Optimization & Information Computing, 10, 457-483.

93. Yousof, H. M., Afify, A. Z., Abd El Hadi, N. E., Hamedani, G. G. and Butt, N. S. (2016). On six-parameter Fréchet distribution: properties and applications. Pakistan Journal of Statistics and Operation Research, 12, 281-299.

94. Yousof, H. M., Afify, A. Z., Nadarajah, S., Hamedani, G. and Aryal, G. R. (2018a). The Marshall-Olkin generalized-G family of distributions with Applications. Statistica, 78, 273-295.

95. Yousof, H. M., Ali, M. M., Hamedani, G. G., Aidi, K. and Ibrahim, M. (2022). A new lifetime distribution with properties, characterizations, validation testing, different estimation methods. Statistics, Optimization & Information Computing, 10, 519-547.

96. Yousof, H. M., Alizadeh, M., Jahanshahiand, S. M. A., Ramires, T. G., Ghosh, I. and Hamedani, G. G. (2017). The transmuted Topp-Leone G family of distributions: theory, characterizations and applications. Journal of Data Science, 15, 723-740.

97. Yousof, H. M., Altun, E., Ramires, T. G., Alizadeh, M. and Rasekhi, M. (2018b). A new family of distributions with properties, regression models and applications, Journal of Statistics and Management Systems, 21, 163-188.

98. Yousof, H. M., Altun, E., Rasekhi, M., Alizadeh, M., Hamedani, G. G. and Ali, M. M. (2019). A new lifetime model with regression models, characterizations and applications. Communications in Statistics-Simulation and Computation, 48, 264-286.

99. Yousof, H. M., Chesneau, C., Hamedani, G. and Ibrahim, M. (2021). A new discrete distribution: properties, characterizations, modeling real count data, Bayesian and non-Bayesian estimations. Statistica, 81, 135-162.